April 24, 1990

LBL--28841

DE91 001792

U(1)′ Dark Matter and R-Parity Violation*

David Ernest Brahm

Ph. D. Dissertation

Physics Department, University of California, Berkeley, CA 94720,

and

Theoretical Physics Group, Lawrence Berkeley Laboratory,

1 Cyclotron Rd., Berkeley, CA 94720

*This work was supported in part by the Director, Office of Energy Research, Office of High Energy and Nuclear Physics, Division of High Energy Physics of the U.S. Department of Energy under Contract DE-AC03-76SF00098 and in part by the National Science Foundation under grant PHY85-15857.

U(1)′ Dark Matter and R-Parity Violation

by

David E. Brahm

Physics Department, University of California, Berkeley, CA 94720,

and

Theoretical Physics Group, Lawrence Berkeley Laboratory

1 Cyclotron Rd., Berkeley, CA 94720

ABSTRACT

Attempts to understand physics beyond the Standard Model must face many phenomenological constraints, from recent Z^0 data, neutral current measurements, cosmology and astrophysics, neutrino experiments, tests of lepton- and baryon-number conservation and CP violation, and many other ongoing experiments. The most interesting models are those which are allowed by current data, but offer predictions which can soon be experimentally confirmed or refuted. Two classes of such models are explored in this dissertation. The first, containing an extra U(1)′ gauge group, has a dark matter candidate which could soon be detected. The second, incorporating supersymmetry with R-parity violation, predicts rare Z^0 decays at LEP; some of these models can already be ruled out by LEP data and gluino searches at the Tevatron.

For my parents,

who did most of the work

Acknowledgements

For the doom of Man is that he forgets.
– Merlin the Magician, "Excalibur"

My deepest thanks and admiration go to my advisor, Prof. Lawrence J. Hall, whose wisdom, insight, and patience made this dissertation possible. He has tried to teach me to see the physics of a problem, to reach an understanding of the whole before getting lost in the details, and he has set an example which I will always try to follow.

I also wish to thank the many other physicists who patiently helped me with this work, including Mahiko Suzuki, Mike Barnett, Bob Cahn, Bernard Sadoulet, Riccardo Barbieri, Gian Giudice, and Jim Freeman. Many of the ideas here stem from discussions with my friends and colleagues Steve Hsu, Eric Carlson, Josh Burton, Greg Anderson, Kim Griest, and Fred Kral. Thanks and condolences go to my dissertation committee, Lawrence Hall, Mahiko Suzuki, and Henry Helson, for reading and commenting on this work in its various stages. Everyone knows the real work is done by the secretaries, Betty Moura and Luanne Neumann at L.B.L.; and Ken Miller, Anne Takizawa, and Donna Sakima on campus.

Thanks of a more personal nature go to Karen Hunold, whose love has given me strength and serenity through this whole project; to Brother Robert Sullivan, who introduced me to the joy of physics; and to my parents, who have encouraged and supported me throughout my academic career.

CONTENTS

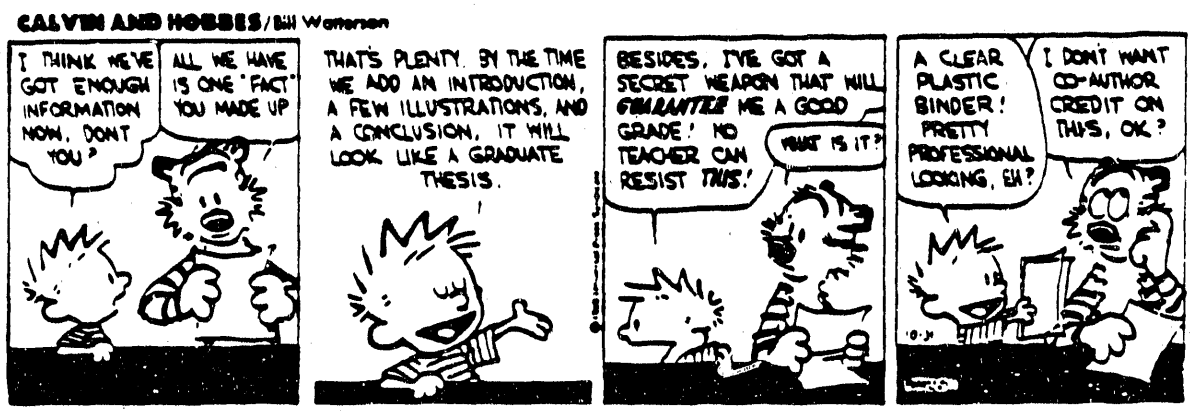

I. PHENOMENOLOGY IN THE PRE-SSC ERA

All we've got is this moment, the 21st Century's yesterday.
– INXS, "Need You Tonight"

A. WHERE DO WE GO FROM HERE?

The success of the $SU(3)_C \otimes SU(2)_W \otimes U(1)_Y$ Standard Model in the 1970's and 1980's provided a welcome understanding of the profusion of "elementary" particles then known. All experimental data to this day has proven consistent with the Standard Model, and of the 18 free parameters in the theory (3 coupling constants, 10 masses, 4 Kobayashi-Maskawa angles, and the Higgs vev), only the masses of the top and the Higgs have not yet been determined. We need to better understand the non-perturbative aspects of the theory, notably low-energy QCD and topological effects, but this seems largely a matter of developing better mathematical tools. We need to confirm the existence of the top quark and the Higgs boson, but this seems just a matter of building a large enough accelerator (such as the Superconducting Supercollider). A generation of physicists has grown up with no inexplicable data to ponder, no experimental signpost pointing to fundamentally new understanding.

Faced with this situation, physicists have taken several different routes. Some work on the poorly-understood aspects of the Standard Model mentioned above. Some are trying to incorporate quantum gravity, presumably at the experimentally unattainable Planck scale. Some look to the cosmos for unsolved problems, such as inflation, dark matter, and the solar neutrino dearth, which may point the way to new physics. Finally, some try to build larger models which encompass the Standard Model, and which predict new physics just around the corner.

There are esthetic reasons to believe in physics beyond the Standard Model. Perhaps the most compelling is the hierarchy problem, the vast gap between the

weak scale ($\sim$ 100 GeV) and the Planck scale (or the GUT scale), which seems to require an extreme fine-tuning of the Higgs mass. Technicolor theories avoid this problem by doing away with fundamental scalars, replacing them with fermion condensates. Supersymmetry (SUSY), on the other hand, provides for cancellation of scalar and fermion loops above the SUSY-breaking scale, relaxing the need to fine-tune the Higgs mass. Since SUSY must be broken near the weak scale, one may still ask why this lies so far below the Planck scale, but supergravity theories provide some motivation here. At present there is no complete technicolor model which agrees with experiment, so many theorists believe supersymmetry must appear at energies below a TeV.

Another reason to expect physics beyond the Standard Model is the apparent running of the gauge couplings towards a single value at very high energies ($\sim 10^{16}$ GeV), suggesting that a simple gauge group describes physics above this "grand unification" (GUT) scale. Embedding the Standard Model gauge group in a simple GUT group would also explain why hypercharges are discrete. Such discreteness, as manifested in the neutrality of the hydrogen atom and the cancellation of triangle anomalies, cannot be explained in a model with a U(1) factor. The first, and simplest, proposed GUT group was SU(5), which gave predictions for proton decay and the Weinberg angle which are now experimentally ruled out. It is too often overlooked, however, that a supersymmetric SU(5) theory correctly predicts the Weinberg angle, and predicts a slower proton decay rate which is not ruled out by experiment.

Cosmology and astrophysics have also provided motivation for physics beyond the Standard Model. Most compelling in this area is the evidence for non-baryonic dark matter. From galactic rotation curves, we know there is far more mass in galaxies than can be accounted for by luminous stars; at least one-fifth of the mass

needed, in fact, to close the universe (i.e. $\Omega \geq .2$). Theoretical prejudice, for example from inflationary models of the early universe, would place $\Omega = 1$, but that is 100 times more mass than we see in luminous stars. Furthermore, the success of standard nucleosynthesis calculations precludes the possibility that this missing mass is baryonic, so we are forced to conclude that 99% of the universe consists of some "dark matter" which is not in the Standard Model!

These reasons to believe in physics beyond the Standard Model are very non-specific in their predictions, leaving model-builders tremendous leeway. However, it is not easy to write down a new model which addresses the above issues, yet is close enough to the Standard Model at low energies to be consistent with all known experiments. It is even harder to develop such a model with interesting and attainable experimental predictions for the near future. The SSC will almost certainly shed some light on the future direction of physics, but we of the Pre-SSC Era must make do with the experiments we have.

The next section gives a brief overview of some experimental constraints every model must face. The following chapters describe two classes of models which are currently allowed, but make predictions which will soon be verifiable. The first, containing an extra $U(1)'$ gauge group, has a dark matter candidate which could soon be detected. The second, incorporating supersymmetry with R-parity violation, predicts rare Z^0 decays at LEP; some of these models can already be ruled out by LEP data and gluino searches at the Tevatron.

B. EXPERIMENTAL CONSTRAINTS

What follows is necessarily a cursory and incomplete listing of some important phenomenological constraints (as of April 1990) which any model must respect. Far more information and references can be found in the Particle Data Book[1].

1. Z^0 Mass, Width, and Decays

One exciting recent development in experimental high energy physics is the production of $\sim 10^5$ Z^0's (by the end of 1989) at LEP (CERN), with up to 10^7 expected in the near future. Combined results from ALEPH, L3, OPAL and DELPHI[1] for the Z^0 mass ($90.9 \pm .4$ GeV) and width ($2.534 \pm .027$ GeV) tightly constrain $\sin^2\theta_W$ and ρ, and limit the number of new particles lighter than $M_Z/2$. In particular, the number of light neutrino species, $N_\nu = 3.10 \pm .09$, casts strong doubt on the existence of a fourth generation.

No new particles have been seen in Z^0 decays, so any postulated visible particle which couples to the Z^0 (such as a SUSY chargino) must be heavier than 45 GeV. The branching ratios for $Z^0 \to e^+e^-$, $Z^0 \to \mu^+\mu^-$, and $Z^0 \to \tau^+\tau^-$ have confirmed the principle of universality. A lower limit of 24 GeV has been placed on the Standard Model Higgs mass[2] from non-observation of the decay $Z^0 \to h^0\nu\bar{\nu}$. Searches for $Z^0 \to hA$ and $Z^0 \to Z^*h$, where h and A are the lightest scalar and pseudoscalar Higgs fields of supersymmetry, are powerful tests of the Minimal Supersymmetric Standard Model.

A similar wealth of data on $W^\pm$ physics should become available when LEP II begins operation.

2. Neutral Currents

Measurements of neutral-current cross-sections[3], notably neutrino scattering from isoscalar nuclei, accurately determine the Weinberg angle, $\sin^2\theta_W = 0.228 \pm .004$ and the ρ parameter, $\rho = 1.001 \pm .007$. A comparison with the results from the Z^0 and $W^\pm$ masses and the Z^0 width puts an upper limit on the top quark mass, $m_t < 168$ GeV. The value for $\sin^2\theta_W$ is inconsistent with the standard SU(5) theory, but agrees with the supersymmetric SU(5) prediction. $\rho \approx 1$ indicates

that electroweak symmetry breaking occurs predominantly through Higgs doublets. These results also constrain the mass of a Z′ boson and its mixing $\theta_{\rm mix}$ with the Z^0; while the constraints are model-dependent, we have roughly $M_{Z'} > 129\,\mathrm{GeV}$ and $|\theta_{\rm mix}| < 0.20$.

The GIM mechanism insures that neutral currents are flavor-conserving in the limit of degenerate quark masses, correctly predicting the rarity of such flavor-changing neutral current (FCNC) processes as $K_L \to \mu^+\mu^-$ and $K^\pm \to \pi^\pm\bar{\nu}\nu$. The strangeness-changing $K_L - K_S$ mass difference is also a calculable GIM violation which arises from the charm quark mass. Theories of physics beyond the Standard Model often fail because they predict unacceptable flavor-changing neutral currents.

3. Cosmological Constraints

Assuming a big-bang scenario for the early universe, all particle species initially existed in thermal equilibrium number densities. Massless or light stable particles (*e.g.* photons, light neutrinos) would today have a number density $n_0 \approx T_0^3$, where $T_0 = 2.7\,\mathrm{K}$. From this we calculate $\Omega_\gamma = 10^{-5}$ in photons, and if neutrinos had a mass of 65 eV we would find $\Omega_\nu = 1$. The equilibrium number density of a heavier stable particle would decrease rapidly as the universe cooled below the particle's mass, but at some point the particles would fail to annihilate rapidly enough to maintain thermal equilibrium, and would "freeze out". A Lee-Weinberg calculation of the present mass density then gives roughly $\Omega \approx (10^{-9}\,\mathrm{GeV}^{-2})/\langle\sigma_A v\rangle$; *e.g.* a 4 GeV neutrino would also give $\Omega_\nu = 1$. These two dark matter candidates, an 65 eV neutrino and a 4 GeV neutrino, typify "hot" and "cold" dark matter. Masses in between are forbidden by astrophysical measurements of the deceleration parameter q_0, giving $\Omega \leq 2$.

Standard nucleosynthesis calculations correctly predict the current abundances

of light elements. These calculations require the universe to be radiation dominated in the MeV era, limit the number of light ($<$ MeV) particle species, and tightly constrain the current baryon number density ($n_B/n_\gamma = 3 \times 10^{-10}$). The latter provides a strong argument against baryonic dark matter. The source of the baryon asymmetry is still a mystery, but it is known that baryogenesis requires a non-equilibrium CP- and B-violating process. The decay of superheavy GUT particles provides such a process, but if this decay occurs too early, any asymmetry would be wiped out by inflation.

If a Lee-Weinberg calculation for a hypothetical particle predicts $\Omega \approx 1$, it is tempting to postulate that the particle constitutes the galactic halos, so that its local density ($0.3\,\mathrm{GeV/cm^3}$) and velocity ($\beta = 10^{-3}$) are known. Dark matter detectors then tightly constrain its interaction cross-section with ordinary nuclei; for dark matter particles of mass 10 GeV to 10 TeV this cross-section must be less than a picobarn. A fourth-generation Dirac neutrino between 10 GeV and 1.4 TeV thus cannot constitute the halo.

Phase transitions which occurred as the universe cooled could strongly influence the mass distribution today. A phase transition could be responsible for inflation, which solves the horizon, flatness, and monopole problems. Topological defects which arise from post-inflation phase transitions, such as domain walls and GUT-scale monopoles, generally overclose the universe, but cosmic strings are allowed and could explain the seeding of galaxies. The effects of the QCD phase transition (~ 200 MeV) are still not well understood, though it is postulated that quark nuggets or black holes could be formed in the process.

Recent COBE data shows the microwave background is extremely uniform, and precisely fits a blackbody spectrum. Particles, hypothetical or known, which would decay after the photon decoupling must not alter this spectrum. These data also

show that structure (*i.e.* proto-galaxies and galactic clusters) did not appear until after the eV-era ($Z = 3000$), yet large-scale maps of the universe show walls and bubble-like structures out to hundreds of megaparsecs today, and quasars which formed as early as $Z = 4.7$. The distribution of matter in the universe appears to be inconsistent with hot dark matter, and may not agree with cold dark matter, either. Fermionic hot dark matter (*e.g.* 65 eV neutrinos) is also disfavored because dwarf galaxy halos appear to contain more mass than would be allowed by Fermi statistics.

Though the microwave background contains most of the electromagnetic energy density in the universe, diffuse background radiation has been measured over much of the spectrum. There appears to be more X-ray background than can be accounted for from known X-ray sources, providing a fertile ground for particle theory speculation. On the other hand, any model with decaying hypothetical particles must avoid producing more X-ray and gamma background than is observed.

The completion of the Keck Observatory, and the launch of the Hubble Telescope in April 1990, should vastly improve our knowledge of the large-scale structure and contents of the universe.

4. Astrophysical Constraints

Models of the sun, which incorporate data from helioseismology, sunspot cycles, and geological records of solar luminosity, predict a rate of neutrino output which is several times larger than observed. One explanation is the cooling of the sun's core by hypothetical WIMP's (Weakly Interacting Massive Particles), which are called cosmions if they also constitute the dark matter. Cosmions are nearly excluded now by dark matter detector experiments. Proposed new particles must, of course, avoid cooling stars too much. Many models with Majorons (the Goldstone bosons of

broken lepton number) fail because Majorons cool red giants; the solution is usually to give the Majorons a mass.

Other solutions to the Solar Neutrino Problem provide grist for the theory mill. An example is the MSW effect, in which neutrinos change species as they pass through the sun. Detection of lower-energy neutrinos will soon test this idea.

The supernova SN1987A provided data on the neutrino output, luminosity curve, and structure of Type II supernovas. About 10^{58} neutrinos $\times$ 6 species, of average energy 10 MeV, should have been produced, carrying away most of the star's original gravitational energy. The detection of about 10 $\bar{\nu}_e$'s at Kamiokande and IMB confirms this prediction, supporting our models of supernova physics, and limiting the amount of energy which could have been carried off by right-handed neutrinos and other hypothetical particles. This argument gives a provisional limit of $\mu_\nu \lesssim 10^{-13}\mu_B$ on neutrino magnetic moments*, suggesting Dirac masses $\lesssim 2$ keV. Arrival time data put limits on the electron neutrino mass, and constrain the decay modes of neutrinos. For example, if the decay $\nu_\mu \rightarrow \nu_e\gamma$ occurred within the supernova, the luminosity would have been greater, while if it occurred between the supernova and here, a cosmic background of such photons would have been detected.

5. Neutrinos

Any non-zero neutrino mass requires physics beyond the Standard Model, either a new particle (ν^c) or lepton-number violation. Neutrino masses are currently limited to 18 eV (ν_e, from tritium decay), 250 keV (ν_μ, from π-decay kinematics), and 35 MeV (ν_τ, from τ-decay kinematics). One experiment at ITEP stubbornly continues to report a value $m(\nu_e) = 25$ eV. Searches for neutrino-less double-β decay constrain the majorana mass of ν_e to be less than 2 eV.

*The cooling rate for red giants gives a more model-independent limit of $\mu_\nu \lesssim 10^{-11}\mu_B$.

Much stronger constraints on neutrino masses and lifetimes come from cosmology, supernova and red giant physics, pion decay ($\pi \rightarrow e\nu_\tau$), and gamma ray background; from these arguments neutrinos above 65 eV are excluded under very general assumptions. Neutrino oscillation searches at nuclear reactors, at accelerators, in the atmosphere, and in the sun constrain mixing angles and mass-squared differences between generations. Many ambitious plans have been made for more sensitive neutrino detectors in the near future.

6. Lepton- and Baryon-Number Conservation

While the Standard Model incorporates lepton- and baryon-number conservation automatically, most new theories must impose one or the other by hand (such as R-parity), or explain why they are so small. Liquid scintillation detectors have so far failed to observe proton decay (*i.e.* $p \rightarrow e^+\gamma$ or $p \rightarrow \pi^+\bar{\nu}$), placing a lower limit of about 10^{32} y on the proton lifetime. The non-observation of processes such as $\mu^- \rightarrow e^-\gamma$ or $K_L \rightarrow \mu^+e^-$ show that lepton number is highly conserved, while searches for neutron oscillations and nuclear decays show that baryon number is highly conserved.

Note, however, that violation of a single generation of lepton number, *i.e.* only electron number, would not permit any of the above processes, so it is not so tightly constrained. However, in this case the electron neutrino would acquire a Majorana mass, so neutrino mass limits provide constraints. Forward-backward asymmetries in e^+e^- collisions, Bhabha scattering, and muon decay also constrain the violation of a single family number.

7. CP Violation

In the Standard Model, CP violation arises from a phase δ in the Kobayashi-Maskawa matrix, and from the $\theta_{\rm QCD}$ parameter.

Prediction of CP violation from δ requires knowledge of the other Kobayashi-Maskawa mixing angles, which are found from various decay rates (including B-mesons), deep inelastic neutrino scattering, and the unitarity condition. CP violation is seen in kaon decays. ϵ characterizes CP violation in $K^0 - \bar{K}^0$ mixing $[\mathcal{O}(G_F^2)]$, while ϵ' measures CP violation in decay amplitudes $[\mathcal{O}(G_F)]$. Measurements of ϵ and ϵ' constrain CP violation arising from new physics; for example, models with a charged Higgs have CP-violating contributions from diagrams in which $W^\pm$ is replaced by $h^\pm$. Further information on CP violation may come soon from studies of $B - \bar{B}$ mixing and B-meson decays.

CP violation arises in QCD from an anomaly in the $\mathrm{U(1)_A}$ rotation needed to make the quark mass matrix real, and is characterized by a parameter θ_{QCD}. However, limits on the neutron electric dipole moment ($d_n < 10^{-25}\,\mathrm{e-cm}$) show that $\theta_{\mathrm{QCD}} < 10^{-8}$ (the "strong CP problem"). One possible explanation is that $m_u = 0$, but this appears to conflict with K and π mass measurements. Another requires two Higgs doublets (as in supersymmetry), with a global Peccei-Quinn symmetry. SU(3) instantons break the $\mathrm{U(1)_{PQ}}$, and drop θ_{QCD} to a CP-conserving minimum. However, the pseudo-Goldstone bosons of broken $\mathrm{U(1)_{PQ}}$, called axions, are disallowed at the electroweak scale by direct searches, and at many other scales by astrophysical and cosmological arguments. Negative axion searches now force models of new physics to avoid a PQ symmetry. In supersymmetry, a $\mu H_1 H_2$ term (needed for proper electroweak breaking) breaks $\mathrm{U(1)_{PQ}}$.

8. QCD and Hadronic Physics

At short distances, perturbative QCD can be studied in deep inelastic scattering and high-energy hadron collisions to determine Λ_{QCD}. Our understanding of bound systems is poorer, though helped in part by bag models, the chiral Lagrangian

formalism, and lattice QCD studies. Experiments at the Tevatron (Fermilab)[4,5] have placed lower limits on the top quark mass (89 GeV), gluino masses (74 GeV), and squark masses (150 GeV). Since many experiments necessarily involve QCD interactions (particularly at hadron colliders!), a better understanding of QCD would greatly improve our ability to probe physics beyond the Standard Model.

II. U(1)′ DARK MATTER

Twinkle, twinkle, little star, / How I wonder what you are!
– "The Star" (Jane Taylor)

A. INTRODUCTION

In addition to their Standard Model interactions, the known quarks and leptons may interact via gauge bosons somewhat heavier than the $W^{\pm}$ and Z^0. Such extra gauge bosons can be sought in particle accelerators, *e.g.* by direct production at e^+e^- or hadron colliders, or by measuring deviations from Standard Model predictions for neutral current and charged current phenomena. In this chapter we demonstrate that present and future dark matter detectors provide powerful, indirect probes for a Z′. Furthermore, searches can cover a large mass range, $M_Z < M_{Z'} \leq 2\,\mathrm{TeV}$.

This probe rests on the assumption that the dark matter is a neutral Dirac fermion ψ, which interacts with ordinary matter only through the Z′, with coupling strength

$$G' = \frac{\sqrt{2}}{8}\frac{(g_1')^2}{M_{Z'}^2} \tag{II.A.1}$$

A freezeout calculation gives a relic abundance for ψ of approximately

$$\Omega_\psi = \frac{(1/66\,\mathrm{TeV})^2}{\langle\sigma_A v\rangle\, h_0^2} = 1 \tag{II.A.2}$$

where

$$\langle\sigma_A v\rangle \sim (G')^2 m_\psi^2 \qquad (m_\psi < M_{Z'}) \tag{II.A.3a}$$

$$\langle\sigma_A v\rangle \sim (g_1')^4/m_\psi^2 \qquad (m_\psi > M_{Z'}) \tag{II.A.3b}$$

and $h_0 = \frac{1}{2}$. Constraining $g_1' < \sqrt{4\pi}$ limits us to the region $1\,\mathrm{GeV} < m_\psi < 40\,\mathrm{TeV}$.

This dark matter could be directly seen by germanium[6,7] (or superconducting granule[8]) detectors, which register the nuclear recoil from an elastic collision between ψ and a nucleus. The coherent elastic scattering cross-section from Z′ exchange is:

$$\sigma_{\rm el} \sim \frac{(G')^2 m_\psi^2 A^2}{(1+m_\psi/M_{\rm Ge})^2} \qquad \text{(II.A.4)}$$

where A is the atomic weight and $M_{\rm Ge}$ is the mass of the nucleus. This is correct even for $m_\psi > M_{Z'}$, since the momentum transfer is low. Eqs. (II.A.2), (II.A.3a), and (II.A.4) combine to give:

$$\sigma_{\rm el} \sim \frac{1}{(1+m_\psi/M_{\rm Ge})^2} \qquad (m_\psi < M_{Z'}) \qquad \text{(II.A.5a)}$$

$$\sigma_{\rm el} \sim m_\psi^2 \,/\, M_{Z'}^4 \qquad (m_\psi > M_{Z'} > M_{\rm Ge}) \qquad \text{(II.A.5b)}$$

Thus, for $m_\psi < M_{Z'}$, $\sigma_{\rm el}$ is large and constant when $m_\psi < M_{\rm Ge}$, then drops as $1/m_\psi^2$ at larger values. $\sigma_{\rm el}$ increases again (as m_ψ^2) for $m_\psi > M_{Z'}$, so it is possible to get observable signals over large ranges of m_ψ and $M_{Z'}$. Our calculations show the most likely regions for observable signals are:

I. $\quad 10\,\text{GeV} < m_\psi < 100\,\text{GeV} \qquad (m_\psi < M_{Z'})$

II. $\quad 400\,\text{GeV} < m_\psi < 40\,\text{TeV} \qquad (m_\psi > M_{Z'})$

In this introduction we have argued that experiments searching for elastic scattering of dark matter particles may allow for a probe of a new U(1)′ gauge interaction. After an overview of some U(1)′ models in Section B, we calculate cross-sections in Section C for both Dirac and Majorana fermions. The results for Dirac fermions (Sections C.1 and C.2) are close to experimental limits. In Sections D and E we look at additional model-dependent constraints, and our results are summarized in Section F.

B. U(1)′ MODELS

1. A Prototype U(1)′

The choice of a U(1)′ will affect our final result for σ_{el} by a small multiplicative factor Φ, generally in the range $\frac{1}{2} \leq \Phi \leq \frac{3}{2}$ (though $\Phi \ll 1$ in cases of accidental cancellation of the proton and neutron charges). We choose in this subsection a prototype U(1)′, for which we take $\Phi \equiv 1$.

Consider $SO(10) \rightarrow SU(5) \otimes U(1)_X$. The SU(5) is taken to be the usual Georgi-Glashow model, and we break $U(1)_X$ at roughly the TeV scale with a Higgs ϕ (from a $\overline{16}$). Our prototype U(1)′ is then just $U(1)_X$, whose normalized charge is

$$S^{(1)} = \sqrt{\tfrac{5}{8}}\,(B\text{-}L - \tfrac{4}{5}Y) \qquad \text{(II.B.1)}$$

In addition to the 15 Standard-Model Weyl spinors (Q, U^c, D^c, L, and E^c), the $\underline{16}$ of SO(10) contains an N^c which transforms under $SU(5) \otimes U(1)_X$ as $(\underline{1}, \sqrt{\frac{5}{8}})$. A term $\phi N^c N$ couples N^c to an SO(10) singlet N, giving rise to a Dirac fermion

$$\psi = \begin{pmatrix} \bar{N} \\ N^c \end{pmatrix} \qquad \text{(II.B.2)}$$

ψ is our dark matter candidate, coupling to ordinary matter only through the exchange of a TeV-scale Z′.

We omit all couplings like LN^ch^c which would make ψ unstable, by imposing some discrete symmetry (*e.g.* $N \rightarrow iN$, $N^c \rightarrow -iN^c$). One can view such an SO(10)-violating discrete symmetry two ways. The first is to simply accept the low-energy model as it stands, with Yukawa couplings

$$\mathcal{L} = QU^ch^c + QD^ch + LE^ch + \phi N^cN \qquad \text{(II.B.3)}$$

and with the gauged $U(1)_X$, without worrying about GUT embeddings (or even supersymmetry). The second is to invoke the Hosotani breaking mechanism, in

which Yukawa couplings do not maintain the expected relations, and may vanish by a discrete symmetry or for topological reasons.[9]

Another possibility we will consider, in the absence of the SO(10) singlet N, is that N^c forms a Majorana fermion. Since Majorana fermions only have axial vector couplings, they are much harder to detect.

2. Other Popular U(1)'s

Nothing in the calculations of Section C requires unification; however, in order to sample some other U(1)′ theories, we now consider several models which arise from E_6 unification.

When E_6 breaks down

$$E_6 \rightarrow SO(10) \otimes U(1)_\Omega \rightarrow SU(5) \otimes U(1)_X \otimes U(1)_\Omega \qquad \text{(II.B.4)}$$

the known particles can be embedded in three different ways* corresponding to Georgi-Glashow[10], Flipped[11,12], and Doubly-Flipped SU(5)[13] (see Table 1), and in each case different symmetry-breaking mechanisms can lead to different low-energy U(1)′ symmetries. Any anomaly-free U(1)′ can be characterized as $\beta(B-L) + \lambda Y + \kappa P$, where P is a variant of Peccei-Quinn symmetry. $(B-L)$, Y, and P charges for particles in the $\underline{27}$ are shown in Table 2.

Georgi-Glashow SU(5), broken by an adjoint Higgs (or the Hosotani mechanism), has two leftover U(1) symmetries; we must choose one linear combination to be our U(1)′. String phenomenologists have three favorite choices, known variously in the literature as A, B, C[3] or η, χ, I[14] or Y''', Y'', Y'[15]. Model B (χ, Y'') is identical to our prototype $S^{(1)}$, discussed in the previous subsection. Model C (I, Y'),

*In addition to the embeddings of Table 1, one can switch $D^c \leftrightarrow B^c$, $L \leftrightarrow H$, and $N^c \leftrightarrow N$. Under this transformation, our symmetries transform as $S^{(1)} \leftrightarrow S^{(2)}$, $S^{(3)} \leftrightarrow S^{(3)}$, $S^{(4)} \leftrightarrow S^{(6)}$, $S^{(5)} \leftrightarrow S^{(5)}$, so we do not find any new candidate symmetries this way.

$\underline{27} \to [(\underline{10},-1,1) \oplus (\overline{5},3,1) \oplus (\underline{1},-5,1)] \oplus [(\overline{5},-2,-2) \oplus (\underline{5},2,-2)] \oplus [(\underline{1},0,4)]$						
G-G:	Q, U^c, E^c	D^c, L	N^c	B^c, h	B, h^c	N
1-Flip:	Q, U^c, N^c	U^c, L	E^c	B^c, h^c	B, h	N
2-Flip:	Q, B^c, N	D^c, h^c	N^c	U^c, h	B, L	E^c

Table 1: Particle Assignments for the $\underline{27}$ of E_6

S	β	λ	κ	Q	D^c	U^c	L	E^c	N^c	h	h^c	B	B^c	N	Norm
B-L	1	0	0	$\frac{1}{3}$	$\frac{-1}{3}$	$\frac{-1}{3}$	-1	1	1	0	0	$\frac{-2}{3}$	$\frac{2}{3}$	0	$\sqrt{\frac{3}{8}}$
Y	0	1	0	$\frac{1}{6}$	$\frac{1}{3}$	$\frac{-2}{3}$	$\frac{-1}{2}$	1	0	$\frac{-1}{2}$	$\frac{1}{2}$	$\frac{-1}{3}$	$\frac{1}{3}$	0	$\sqrt{\frac{3}{5}}$
P	0	0	1	$\frac{1}{3}$	$\frac{2}{3}$	$\frac{2}{3}$	1	0	0	-1	-1	$\frac{-2}{3}$	$\frac{-4}{3}$	2	$\sqrt{\frac{3}{20}}$
$S^{(1)}$	5	-4	0	1	-3	1	-3	1	5	2	-2	-2	2	0	$\sqrt{\frac{1}{40}}$
$S^{(2)}$	0	2	5	2	4	2	4	2	0	-6	-4	-4	-6	10	$\sqrt{\frac{1}{160}}$
$S^{(3)}$	10	-6	5	4	-2	4	-2	4	10	-2	-8	-8	-2	10	$\sqrt{\frac{1}{240}}$
$S^{(4)}$	0	-2	1	0	0	2	2	-2	0	0	-2	0	-2	2	$\sqrt{\frac{1}{16}}$
$S^{(5)}$	2	6	1	2	2	-4	-4	8	2	-4	2	-4	2	2	$\sqrt{\frac{1}{96}}$
$S^{(6)}$	1	-2	0	0	-1	1	0	-1	1	1	-1	0	0	0	$\sqrt{\frac{1}{4}}$
$S^{(7)}$	3	0	0	1	-1	-1	-3	3	3	0	0	-2	2	0	$\sqrt{\frac{1}{24}}$

Table 2: Charges for Candidate U(1)′ Symmetries

which we call $S^{(2)}$, is popular because the N^c can take a large Majorana mass and drive the neutrino mass seesaw mechanism; in that case our ψ would have to consist of N (if Majorana), or of N and an E_6 singlet P (if Dirac). Model A (η, Y''', or $Y_E^{[16]}$), which we call $S^{(3)}$, is the only one which arises from Hosotani breaking of E_6 directly to the rank-5 group.

Flipped $SU(5) \otimes U(1)_X$ is broken to the Standard Model with Higgses in the $(\underline{10}, -1)$ and $(\overline{10}, 1)$ representations. Depending on where these Higgses reside in E_6, they can leave different U(1)′ symmetries unbroken. If they come from $\underline{27}$ and $\overline{27}$, they leave symmetry $S^{(4)}$, while if they come from a $\underline{78}$, they leave $S^{(5)}$. Doubly

Flipped $SU(5) \otimes U(1)_X \otimes U(1)_\Omega$ is broken to the Standard Model by Higgses in the $(\underline{10}, -1, 1)$ and $(\overline{10}, 1, -1)$ representations (from $\underline{27}$ and $\overline{27}$), which leave yet another $U(1)'$ candidate, $S^{(6)}$.

Finally, we consider $S^{(7)} = B-L$, which comes, for example, from a Pati-Salam model.[17] Our seven popular $U(1)'$s, with their $[\beta, \lambda, \kappa]$ values, particle charges, and normalizations, are listed in Table 2.

C. CROSS-SECTION CALCULATIONS

1. A Light Dirac Fermion

In this subsection we predict the germanium scattering cross-section for a Dirac fermion with $m_\psi \ll \frac{1}{2} M_{Z'}$. This is the most interesting case, since our results are nearly model-independent and close to experimental limits. ψ must consist of two Weyl spinors of different $U(1)'$ charges; otherwise the calculations of Subsection 3 apply. Under our various candidate symmetries, we could take

$$\psi^{(1),(4),(6),(7)} = \begin{pmatrix} \bar{N} \\ N^c \end{pmatrix}, \qquad \psi^{(2),(3),(5)} = \begin{pmatrix} \bar{N} \\ P \end{pmatrix} \tag{II.C.1}$$

where P is some other particle with zero charge under the relevant symmetry.

ψ interacts with a germanium nucleus via a t-channel Z′ exchange, as in Fig. 1. The effective Lagrangian is:

$$\mathcal{L} = \sqrt{2} G' \bar{\psi} \gamma^\mu (V_\psi - A_\psi \gamma_5) \psi \; \overline{\mathrm{Ge}} \, \gamma_\mu (V_{\mathrm{Ge}} - A_{\mathrm{Ge}} \gamma_5) \mathrm{Ge} \tag{II.C.2}$$

Here $V_\psi = S_L + S_R$ and $A_\psi = S_L - S_R$, where S_L and S_R are the $U(1)'$ charges of ψ_L and ψ_R respectively. V_{Ge} is a sum of constituent charges, so it is of order the atomic weight $A = 72.6$. A_{Ge} (the "Gamow-Teller strength") is a sum of spins, so it is of order the nuclear spin, which is only non-zero for ^{73}Ge with natural abundance of 7.8%. Thus we can ignore A_{Ge} in our calculations.

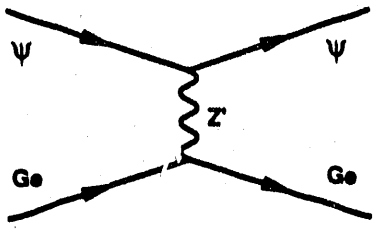

Figure 1: Interaction with Germanium

The Standard-Model neutrino interaction (via the Z^0) can be recovered from (II.C.2) by:

$$\psi \to \nu, \quad G' \to G_F, \quad S_L = \tfrac{1}{2}, \quad S_R = 0, \quad V_{\rm Ge} = (\tfrac{1}{2} - 2\sin^2\theta_W)Z - \tfrac{1}{2}N \quad \text{(II.C.3)}$$

while in our prototype U(1)′ model we have:

$$S_L = S(N^c) = \sqrt{\tfrac{5}{8}}, \quad S_R = -S(N) = 0, \quad V_{\rm Ge} = \sqrt{\tfrac{2}{5}}Z + \sqrt{\tfrac{8}{5}}N = 71.6 \quad \text{(II.C.4)}$$

In the non-relativistic limit, $\sigma_{\rm el}$ is[18]:

$$\sigma_{\rm el} = \frac{2}{\pi}(G' m_\psi V_\psi)^2 \left(\frac{M_{\rm Ge}}{m_\psi + M_{\rm Ge}}\right)^2 V_{\rm Ge}^2 \quad \text{(II.C.5)}$$

where $M_{\rm Ge} = 68\,{\rm GeV}$.

A Lee-Weinberg analysis[19] gives the relic abundance of ψ particles from their annihilation cross-section σ_A. We assume no particle-antiparticle asymmetry for ψ.[20] Define

$$Z \equiv \sqrt{\frac{45}{4\pi^3 g^*}} m_\psi M_P \langle \sigma_A v \rangle, \quad \langle \sigma_A v \rangle \equiv a + bX_F, \quad X_F \equiv T_F/m_\psi \quad \text{(II.C.6)}$$

where g^* is the effective number of relativistic particle degrees of freedom at the freezeout temperature T_F. Above .2 GeV, g^* approximately obeys[21]

$$g^*(T_F) = 90 - \sqrt{(225\,{\rm GeV})/T_F} \quad \text{(II.C.7)}$$

We set

$$\Omega_\psi = \left(\frac{\ln Z}{Z}\right)\left(\frac{12}{g^*}\frac{1}{2.75}\right) T_0^3 m_\psi/\rho_0 = 1 \quad \text{(II.C.8)}$$

The numerical factors in the second term arise from a depletion in g^*, and a consequent rise in temperature, associated with the QCD phase transition and the electron freezeout. This gives

$$a + \tfrac{1}{2} b X_F = (9.28 \times 10^{-10}\,\mathrm{GeV}^{-2}) \left(\frac{.25}{\Omega h_0^2}\right) \sqrt{\frac{90}{g^*}} \left(\frac{\ln Z}{24}\right) \qquad \text{(II.C.9)}$$

Uncertainty in the normalized Hubble parameter h_0 allows $0.16 \leq \Omega h_0^2 \leq 1$. (If we only require ψ's to constitute the halo, then $0.016 \leq \Omega h_0^2 \leq 0.1$) The value $\Omega h_0^2 = \frac{1}{4}$ is preferred on theoretical grounds tc close the universe and give it a sufficient age for stellar evolution.

The annihilation diagram of Fig. 2 in the non-relativistic limit[18,22] gives

$$\langle \sigma_A v \rangle = \frac{4}{\pi} (G' m_\psi V_\psi)^2 [1 + 2R X_F] \left(\sum_f S_f^2\right) \qquad \text{(II.C.10)}$$

where

$$R = \frac{V_\psi^2 + A_\psi^2}{2V_\psi^2} \qquad \text{(II.C.11)}$$

$R = 1$ in all the models we are considering, and in any case since $X_F = (\ln Z)^{-1} \approx 0.04$, R is unimportant here. The last term in (II.C.10) is a sum of U(1)′ charges over all kinematically allowed final states, three generations of Standard-Model particles except possibly the top quark. In our prototype model, for $m_\psi > m_t$, we have $\left(\sum_f S_f^2\right) = 4.125$.

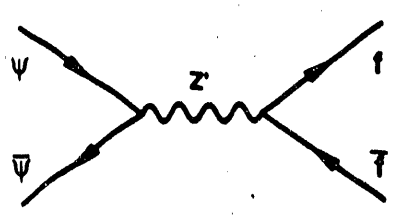

Figure 2: Annihilation Diagram

We put (II.C.10) into (II.C.9), to find that $(G'm_\psi V_\psi)$ is a constant:

$$(G'm_\psi V_\psi)^2 = \frac{7.0\times10^{-10}\,\mathrm{GeV}^{-2}}{\left(\sum_f S_f^2\right)}\left(\frac{.25}{\Omega h_0^2}\right)\sqrt{\frac{90}{g^*}}\left(\frac{\ln Z}{24}\right)\left(\frac{1.04}{1+RX_F}\right) \qquad \text{(II.C.12)}$$

Hereafter we will drop the last term, since it differs negligibly from 1. But now (II.C.5) gives our final result for the germanium cross-section:

$$\sigma_{\mathrm{el}} = (2.15\times10^{-10}\,\mathrm{barns})\,\Phi_d\left(\frac{M_{\mathrm{Ge}}}{m_\psi+M_{\mathrm{Ge}}}\right)^2\left(\frac{.25}{\Omega h_0^2}\right)\sqrt{\frac{90}{g^*}}\left(\frac{\ln Z}{24}\right)\left(\frac{A}{72.6}\right)^2 \qquad \text{(II.C.13)}$$

Φ_d is a numerical factor which depends on the U(1)′ symmetry, and on whether m_ψ lies above or below the top mass; it is normalized to unity for our prototype $S^{(1)}$ in the region $m_\psi > m_t$:

$$\Phi_d \equiv 4.24\,\frac{(V_{\mathrm{Ge}}/A)^2}{\left(\sum_f S_f^2\right)} \qquad \text{(II.C.14)}$$

Values of Φ_d for our candidate symmetries appear in Table 3 (for other U(1)′s see the Appendix).

S	a.k.a.	$\Phi_d^{(<m_t)}$	$\Phi_d^{(>m_t)}$	Υ_d	$\Phi_m^{(<m_t)}$	$\Phi_m^{(>m_t)}$	Υ_m
$S^{(1)}$	B, χ, Y''	1.0378	1.0000	1.0000	1.0378	1.0000	1.0000
$S^{(2)}$	C, I, Y'	0.1228	0.1146	0.0964	4.4198	4.1250	2.3151
$S^{(3)}$	A, η, Y''', Y_E	0.8362	0.6875	0.6547	0.3716	0.3056	0.2528
$S^{(4)}$	1-Flip, $\underline{27}$, $\overline{27}$	0.5858	0.4882	0.5696	0.0000	0.0000	0.0000
$S^{(5)}$	1-Flip, $\underline{78}$	0.6590	0.5858	0.7459	1.3751	1.2222	11.3403
$S^{(6)}$	2-Flip	0.0034	0.0029	0.0034	2.2918	1.9643	5.5061
$S^{(7)}$	$B-L$	1.3744	1.3038	1.4668	0.0000	0.0000	0.0000

Table 3: Multiplicative Factors for Candidate U(1)′ Symmetries

Note our result (II.C.13) depends only on m_ψ (and the U(1)′ factor Φ_d), not on $M_{Z'}$, g_1', or even V_ψ. A plot of σ_{el} vs. m_ψ appears in Fig. 3, for symmetry $S^{(1)}$

and various values of Ωh_0^2. A discontinuity appears at our postulated top quark mass of 100 GeV; we have chosen not to smooth this out so as to show the effect is small. The experimental limits shown are from a germanium detector[6], under the assumption that ψ's have the galactic halo density and velocity distribution. In Fig. 4 we have fixed $\Omega h_0^2 = \frac{1}{4}$, and plotted σ_{el} for the seven candidate U(1)′ symmetries listed in Table 2.

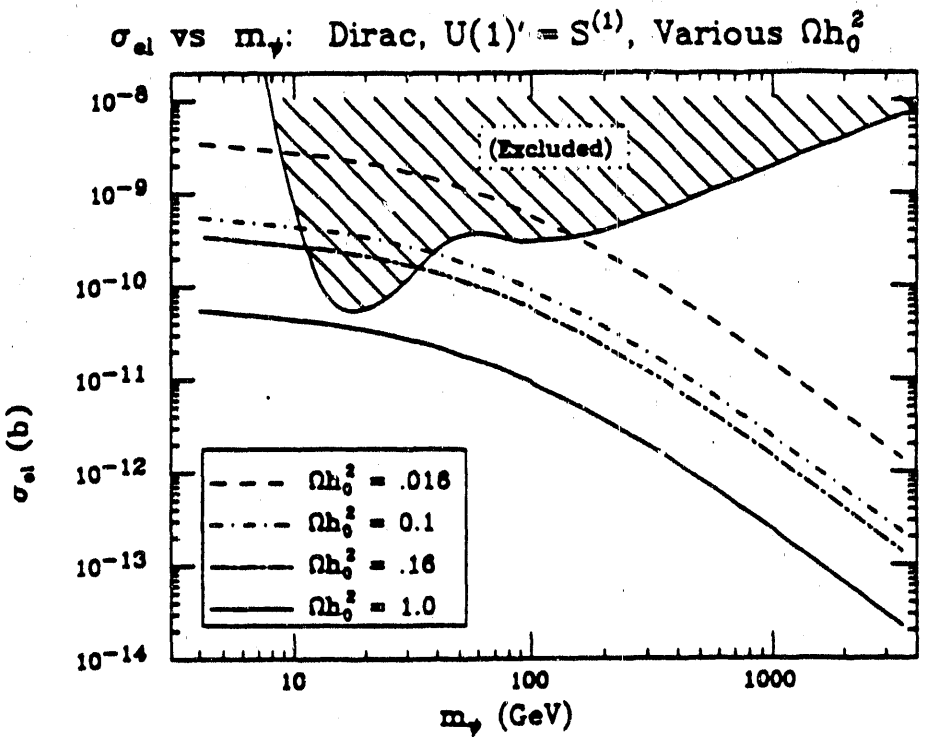

Figure 3: σ_{el} vs. m_ψ: Dirac, $S^{(1)}$, Various Ωh_0^2

For $m_\psi \ll \frac{1}{2}M_{Z'}$, σ_{el} is independent of $M_{Z'}$, g_1', and V_ψ.

Eq. (II.C.12) can be re-written, using prototype values for V_ψ and $\left(\sum_f S_f^2\right)$, as:

$$\frac{(g_1')^2\, m_\psi}{M_{Z'}^2} = (9.3 \times 10^{-5}\,\mathrm{GeV}^{-1})\sqrt{\frac{.25}{\Omega h_0^2}} \qquad \text{(II.C.15)}$$

To keep our U(1)′ in the perturbative regime, we take $g_1' < \sqrt{4\pi}$. For a given $M_{Z'}$, this places a lower limit on m_ψ; for example, if $M_{Z'} = 350\,\mathrm{GeV}$ then $m_\psi > 1\,\mathrm{GeV}$.

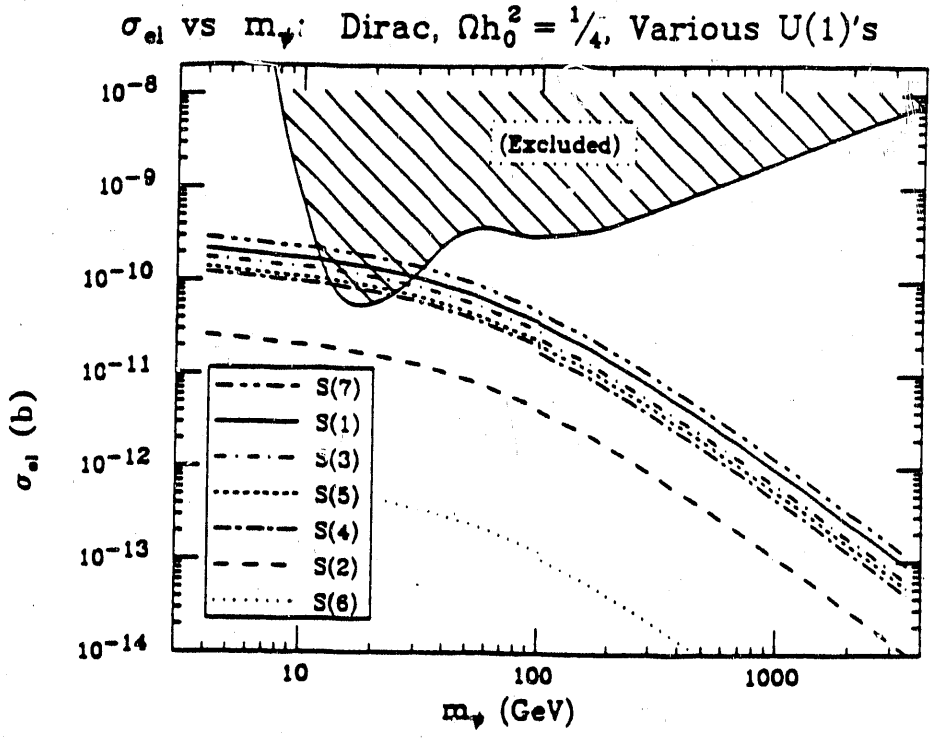

Figure 4: σ_{el} vs. m_ψ: Dirac, $\Omega h_0^2 = \frac{1}{4}$, Various U(1)'s

σ_{el} depends on the U(1)'only through Φ_d, from Table 3.

2. A Heavy Dirac Fermion

Heavier dark matter candidates, with $m_\psi \geq \frac{1}{2} M_{Z'}$, require modification of the above calculations, resulting in a germanium cross-section which now depends on $M_{Z'}$ and V_ψ. Eq. (II.C.10) is modified by the pole factor[18]:

$$P_{Z'} = \frac{M_{Z'}^4}{(4m_\psi^2 - M_{Z'}^2)^2 + \Gamma_{Z'}^2 M_{Z'}^2} \qquad \text{(II.C.16)}$$

For $m_\psi > M_{Z'}$ a new annihilation channel opens, $\psi\bar{\psi} \rightarrow Z'Z'$, from Fig. 5.* In the non-relativistic limit, this contribution is[23]

$$\langle \sigma_A v \rangle_{Z'Z'} = \frac{R^2}{64\pi} \frac{(g_1' V_\psi)^4}{m_\psi^2} \left[\frac{m_\psi (m_\psi^2 - M_{Z'}^2)^{3/2}}{(m_\psi^2 - \frac{1}{2} M_{Z'}^2)^2} \right] \qquad \text{(II.C.17)}$$

where R was defined in (II.C.11). Note the last term goes to unity for $m_\psi \gg M_{Z'}$.

*We assume the U(1)′ Higgs is sufficiently massive to avoid $\psi\bar{\psi} \rightarrow \phi\phi$.

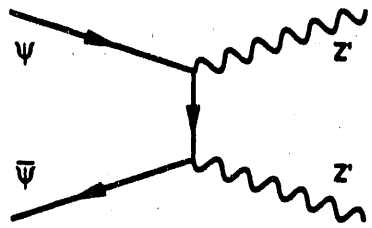

Figure 5: $\psi\bar{\psi} \to Z'Z'$

We combine eqs. (II.C.10), (II.C.16), and (II.C.17) to get the total annihilation cross-section $\langle\sigma_A v\rangle$, then put this in (II.C.9) to get

$$(G' m_\psi V_\psi)^2 = \frac{7.29 \times 10^{-10}\,\mathrm{GeV}^{-2}}{f_d(m_\psi)} \left(\frac{m_\psi}{M_{Z'}}\right)^4 \left(\frac{.25}{\Omega h_0^2}\right) \sqrt{\frac{90}{g^*}} \left(\frac{\ln Z}{24}\right) \qquad \text{(II.C.18)}$$

where

$$f_d(m_\psi) \equiv \frac{m_\psi^4 \left(\sum_f S_f^2\right)(1+RX_F)}{(4m_\psi^2 - M_{Z'}^2)^2 + \Gamma_{Z'}^2 M_{Z'}^2} + \frac{R^2 V_\psi^2}{8} \frac{m_\psi (m_\psi^2 - M_{Z'}^2)^{3/2}}{(m_\psi^2 - \frac{1}{2}M_{Z'}^2)^2} \qquad \text{(II.C.19)}$$

The last term of (II.C.19) vanishes for $m_\psi < M_{Z'}$. Note $f_d(m_\psi \gg M_{Z'}) \to 0.346$ (for $S^{(1)}$), and (II.C.18) reduces to

$$m_\psi = (3. \times 10^3\,\mathrm{GeV})(g_1')^2 \qquad \text{(II.C.20)}$$

The requirement $g_1' < \sqrt{4\pi}$ restricts $m_\psi < 40\,\mathrm{TeV}$.

We combine eqs. (II.C.18) and (II.C.5) to get σ_{el}

$$\sigma_{\mathrm{el}} = (1.24 \times 10^{-11}\,\mathrm{barns}) \left(\frac{m_\psi}{M_{Z'}}\right)^2 \left(\frac{1\,\mathrm{TeV}}{M_{Z'}}\right)^2 U_d\, \Upsilon_d\, \frac{f_d(\infty)}{f_d(m_\psi)} \qquad \text{(II.C.21)}$$

where U_d consists of some factors of unity,

$$U_d \equiv \left(\frac{m_\psi}{m_\psi + M_{\mathrm{Ge}}}\right)^2 \left(\frac{.25}{\Omega h_0^2}\right) \sqrt{\frac{90}{g^*}} \left(\frac{\ln Z}{24}\right) \left(\frac{A}{72.6}\right)^4 \qquad \text{(II.C.22)}$$

Υ_d is a factor which depends on the U(1)′ symmetry, normalized to unity for $S^{(1)}$, and listed for other symmetries in Table 3,

$$\Upsilon_d \equiv 0.356\, \frac{(V_{\mathrm{Ge}}/A)^2}{f_d(\infty)} \qquad \text{(II.C.23)}$$

Thus, the last three terms of (II.C.21) are approximately unity for $m_\psi \gg M_{Z'}$.

Note that we do not include the coherence loss factor η_C[24], since the experimental limits we quote[6] have already accounted for it.

σ_{el} from (II.C.21) is plotted against m_ψ for various values of $M_{Z'}$ in Fig. 6. We have used the prototype symmetry $S^{(1)}$, and taken $\Omega h_0^2 = \frac{1}{4}$.

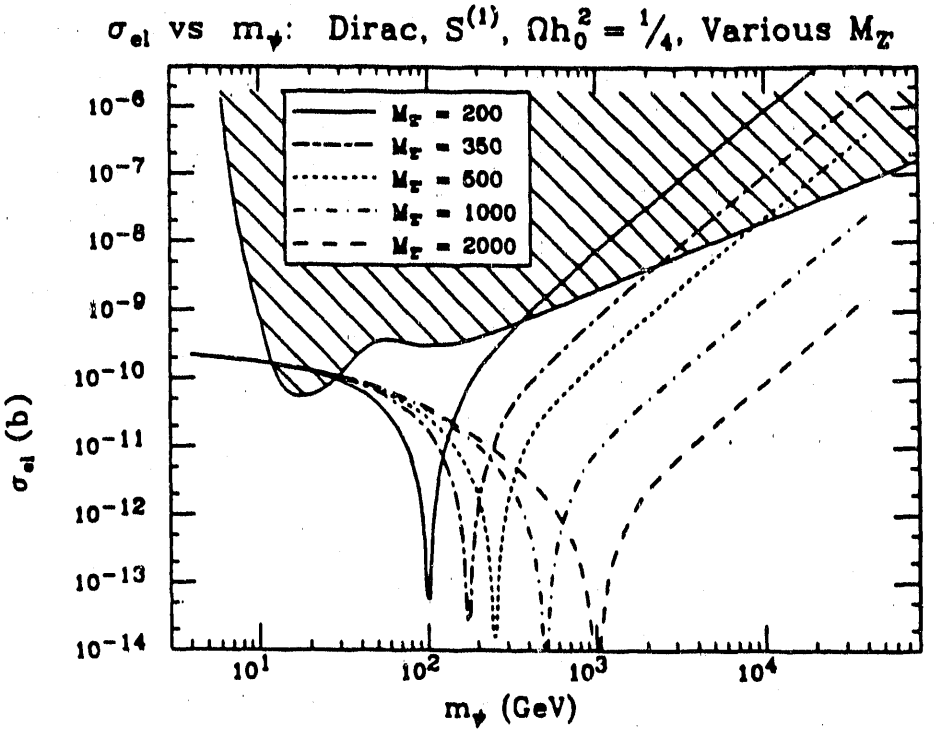

Figure 6: σ_{el} vs. m_ψ: Dirac, $S^{(1)}$, $\Omega h_0^2 = \frac{1}{4}$, Various $M_{Z'}$
In this range σ_{el} depends on $M_{Z'}$.

3. A Light Majorana Fermion

Suppose our prototype model does not contain an N; then in place of eq. (II.B.2) we have a Majorana fermion,

$$\psi = \begin{pmatrix} \bar{N}^c \\ N^c \end{pmatrix} \qquad \text{(II.C.24)}$$

Then [see (II.C.2)] $V_\psi = 0$, $A_\psi = 2S_{N^c}$.* In fact, the calculations of this subsection are valid for any fermion with no vector coupling, such as a ψ of the form (II.B.2) under symmetries $S^{(3)}$ or $S^{(5)}$.

The germanium cross-section is greatly reduced. Eq. (II.C.5) is replaced by[18]

$$\sigma_{\rm el} = \frac{6}{\pi}(G' m_\psi A_\psi)^2 \left(\frac{M_{\rm Ge}}{m_\psi + M_{\rm Ge}}\right)^2 A_{\rm Ge}^2 \qquad \text{(II.C.25)}$$

We take

$$A_{\rm Ge}^2 = (.078)(.37)\,(S_Q + S_{D^c})^2 \qquad \text{(II.C.26)}$$

where the first numerical term is the relative abundance of ^{73}Ge, and the second is from Table III of Goodman and Witten[22]. Note the axial vector strength does not scale as the atomic weight. Thus the Majorana cross-section is over five orders of magnitude smaller than the Dirac case.

The annihilation cross-section [compare to (II.C.10)] is[18]

$$\langle \sigma_A v \rangle = \frac{4}{\pi}(G' m_\psi A_\psi)^2 X_F \left(\textstyle\sum_f S_f^2\right) \qquad \text{(II.C.27)}$$

Combining this with eqs. (II.C.9) and (II.C.25) gives $\sigma_{\rm el}$ [compare to (II.C.13)]:

$$\sigma_{\rm el} = (1.8 \times 10^{-14}\,\text{barns})\,\Phi_m \left(\frac{M_{\rm Ge}}{m_\psi + M_{\rm Ge}}\right)^2 \left(\frac{.25}{\Omega h_0^2}\right) \sqrt{\frac{90}{g^*}} \left(\frac{\ln Z}{24}\right)^2 \qquad \text{(II.C.28)}$$

$$\Phi_m \equiv 41.3\,\frac{(S_Q + S_{D^c})^2}{\left(\sum_f S_f^2\right)} \qquad \text{(II.C.29)}$$

Again, Φ_m is normalized to unity for $S^{(1)}$, and listed for other symmetries in Table 3. Eq. (II.C.28) is plotted for our prototype symmetry, with various values of Ωh_0^2, in Fig. 7. Fig. 8 shows $\sigma_{\rm el}$ for our various U(1)$'$ symmetries, with $\Omega h_0^2 = \frac{1}{4}$ fixed.

*This factor of 2 replaces in a natural way the factor of 4 often put by hand into the cross-sections, *e.g.* in Griest and Sadoulet's Appendix A (ref. [18]).

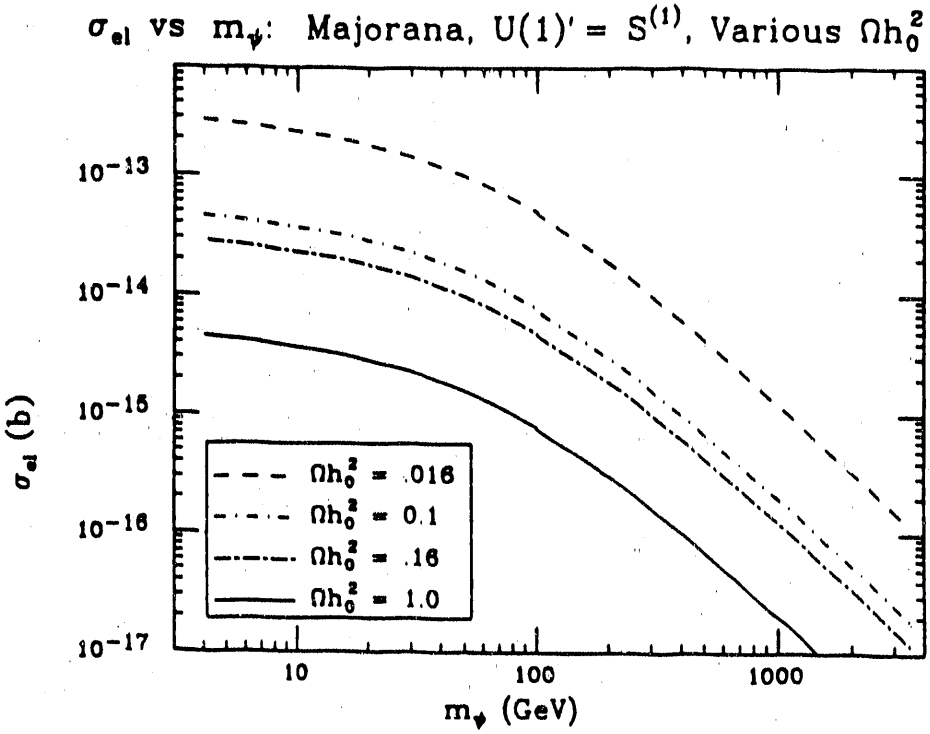

Figure 7: σ_{el} vs. m_ψ: Majorana, $S^{(1)}$, Various Ωh_0^2

These σ_{el}'s are experimentally inaccessible.

4. A Heavy Majorana Fermion

If ψ is Majorana and $m_\psi \geq \frac{1}{2}M_{Z'}$, the annihilation cross-section is[23]

$$\langle \sigma_A v \rangle = \frac{4}{\pi}(G' m_\psi A_\psi)^2 \left(\frac{M_{Z'}}{m_\psi}\right)^4 \times \left[\frac{\left(\sum_f S_f^2\right) X_F\, m_\psi^4}{(4m_\psi^2 - M_{Z'}^2)^2 + \Gamma_{Z'}^2 M_{Z'}^2} + \frac{A_\psi^2}{32}\frac{m_\psi (m_\psi^2 - M_{Z'}^2)^{3/2}}{(m_\psi^2 - \frac{1}{2}M_{Z'}^2)^2}\right] \qquad \text{(II.C.30)}$$

Then eqs. (II.C.9) and (II.C.25) give [compare to (II.C.21)]

$$\sigma_{el} = (8.8 \times 10^{-17}\ \text{barns}) \left(\frac{m_\psi}{M_{Z'}}\right)^2 \left(\frac{1\,\text{TeV}}{M_{Z'}}\right)^2 U_m\, \Upsilon_m \frac{f_m(\infty)}{f_m(m_\psi)} \qquad \text{(II.C.31)}$$

Now $f_m(m_\psi)$ is

$$f_m(m_\psi) \equiv \frac{1}{2}\frac{\left(\sum_f S_f^2\right) X_F\, m_\psi^4}{(4m_\psi^2 - M_{Z'}^2)^2 + \Gamma_{Z'}^2 M_{Z'}^2} + \frac{A_\psi^2}{32}\frac{m_\psi (m_\psi^2 - M_{Z'}^2)^{3/2}}{(m_\psi^2 - \frac{1}{2}M_{Z'}^2)^2} \qquad \text{(II.C.32)}$$

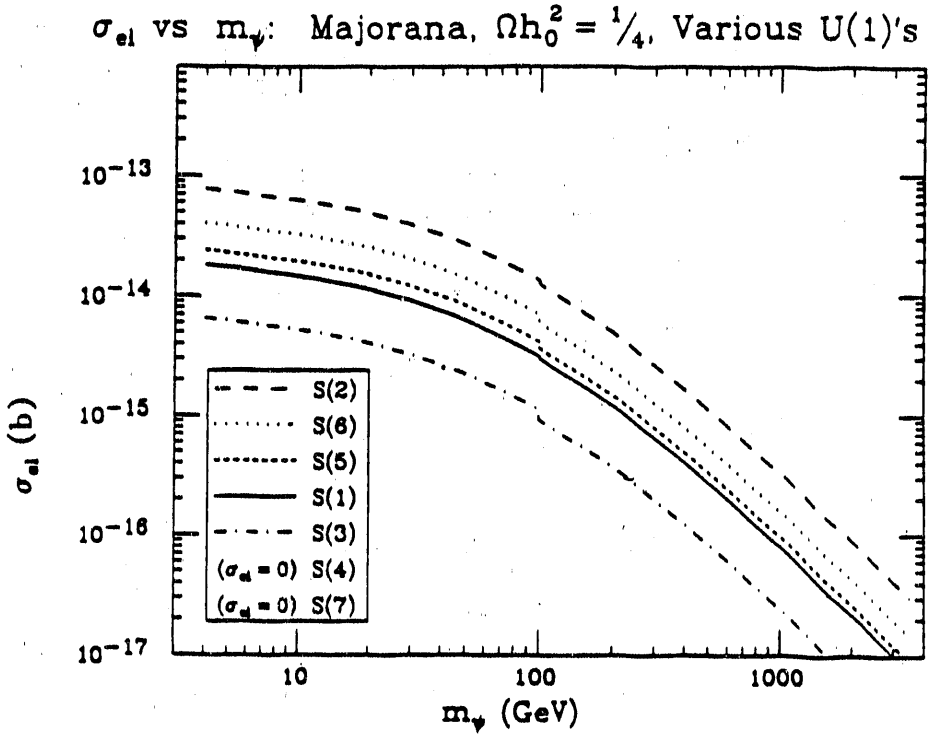

Figure 8: σ_{el} vs. m_ψ: Majorana, $\Omega h_0^2 = \frac{1}{4}$, Various U(1)'s

σ_{el} depends on Φ_m, from Table 3.

(again the last term vanishes for $m_\psi < M_{Z'}$), and U_m consists of some factors of unity,

$$U_m \equiv \left(\frac{m_\psi}{m_\psi + M_{\rm Ge}}\right)^2 \left(\frac{.25}{\Omega h_0^2}\right) \sqrt{\frac{90}{g^*}} \left(\frac{\ln Z}{24}\right) \left(\frac{A}{72.6}\right)^2 \qquad \text{(II.C.33)}$$

Υ_m is a factor which depends on the U(1)′ symmetry, normalized to unity for $S^{(1)}$, and listed for other symmetries in Table 3,

$$\Upsilon_m \equiv 0.833 \, \frac{(S_Q + S_{D^c})^2}{f_m(\infty)} \qquad \text{(II.C.34)}$$

The last three terms of (II.C.31) are approximately unity for $m_\psi \gg M_{Z'}$.

σ_{el} from (II.C.31) is plotted against m_ψ for various values of $M_{Z'}$ in Fig. 9. We have used the prototype symmetry $S^{(1)}$, and taken $\Omega h_0^2 = \frac{1}{4}$.

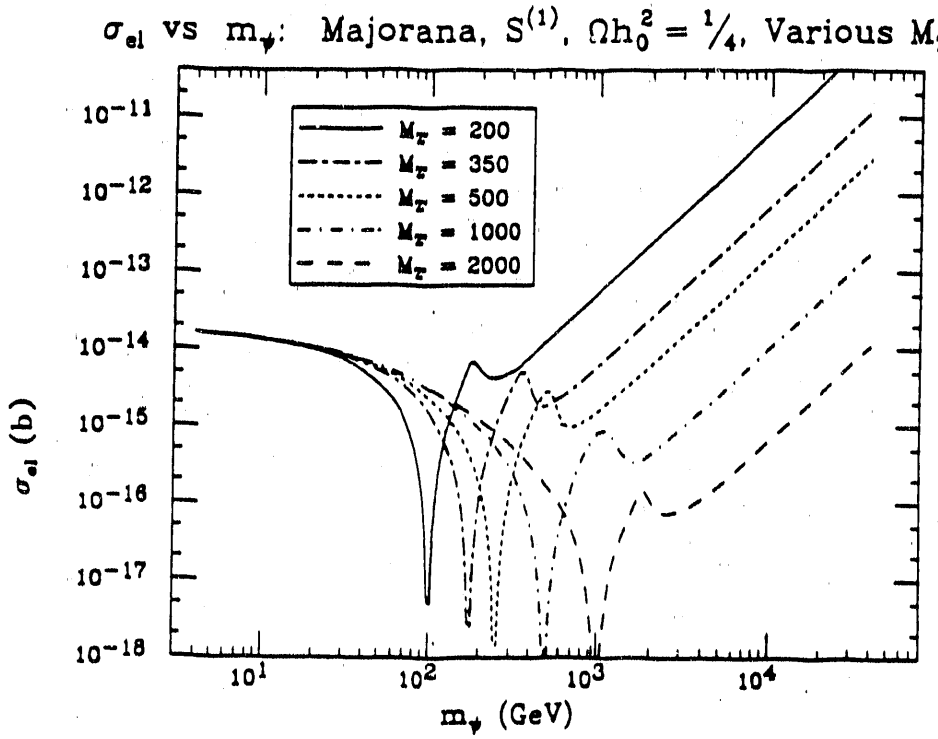

Figure 9: σ_{el} vs. m_ψ: Majorana, $S^{(1)}$, $\Omega h_0^2 = \frac{1}{4}$, Various $M_{Z'}$

D. QUANTUM COMPLICATIONS

Wavefunction and mass mixing between the Z and the Z′ have been studied extensively in the literature,[3,16,25] especially for our first three candidate symmetries [note, however, that mixing does not occur in all models, *e.g.* $S^{(7)}$, pure $B-L$]. Wavefunction mixing, from Fig. 10(a), changes the current to which the Z′ couples, slightly altering the Φ and Υ values given in Table 3. Mass mixing, from Fig. 10(b), introduces a small coupling of ψ to the 91 GeV gauge boson mass eigenstate. Measurements of Standard Model parameters (such as $\rho = 1$) place limits on the Z′ mass and the mixing angle.

Before wavefunction renormalization, let the field A_Y couples to J_Y (hypercharge current) and the field A_X couples to J_X. Mixing will cause A_Y to couple to

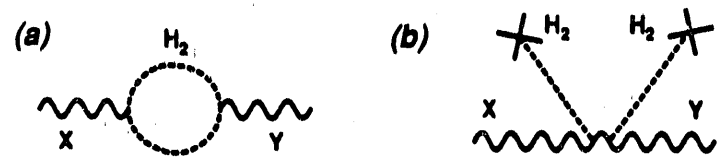

Figure 10: a) Wavefunction Mixing, b) Mass Mixing (H_2 is the doublet Higgs)

$J_Y + \epsilon J_X$ and A_X to couple to $J_X + \epsilon J_Y$, where $\epsilon \approx \frac{g_1^2}{16\pi^2} \ln(M_G/M_{Z'}) \approx 1/20$. The Standard Model B field, which couples to J_Y only, must then be:

$$B = A_Y - \epsilon A_X \tag{II.D.1}$$

and the orthogonal combination, the Z', couples to $J_X + 2\epsilon J_Y$. This changes the ratios λ/β and λ/κ by $\mathcal{O}(2\epsilon)$ for the candidate symmetries we listed in Table 2.

Mass mixing of the Z and Z' is usually studied under the GUT assumption

$$g_1' = g_1 = \sqrt{\frac{5}{3}} \frac{e}{\cos\theta_W} = 0.46 \tag{II.D.2}$$

which is true if $g_1' = g_1$ at the GUT scale and none of the particles in the $\underline{27}$ are heavy. Under these assumptions, and leaving the mixing angle unconstrained, neutral current data and measurements of the Z and W masses (giving $\rho \approx 1$) place lower limits on $M_{Z'}$. We quote the 90% confidence level limits from Costa *et al.*[3], using only the constraint $\rho = 1$, for our first three candidate symmetries:

$$M_{Z'} > 352\,\text{GeV}\,(S^{(1)}), \quad M_{Z'} > 180\,\text{GeV}\,(S^{(2)}), \quad M_{Z'} > 129\,\text{GeV}\,(S^{(3)}) \tag{II.D.3}$$

From the same source, we find limits on the mass mixing angle θ_{mix} (in radians),

$$|\theta_{\text{mix}}| < 0.05\,(S^{(1)}), \quad |\theta_{\text{mix}}| < 0.05\,(S^{(2)}), \quad |\theta_{\text{mix}}| < 0.20\,(S^{(3)}) \tag{II.D.4}$$

As pointed out by Enqvist *et al.*[26], even these small angles can significantly increase $\langle\sigma_A v\rangle$ when $m_\psi \approx M_Z/2$, from the Z^0 resonance. This translates for us into a dip

in our plots of σ_{el} near $m_\psi = 45\,\text{GeV}$. In Fig. 11 we show how Fig. 6 is modified for $\theta_{mix} = 0.03$.

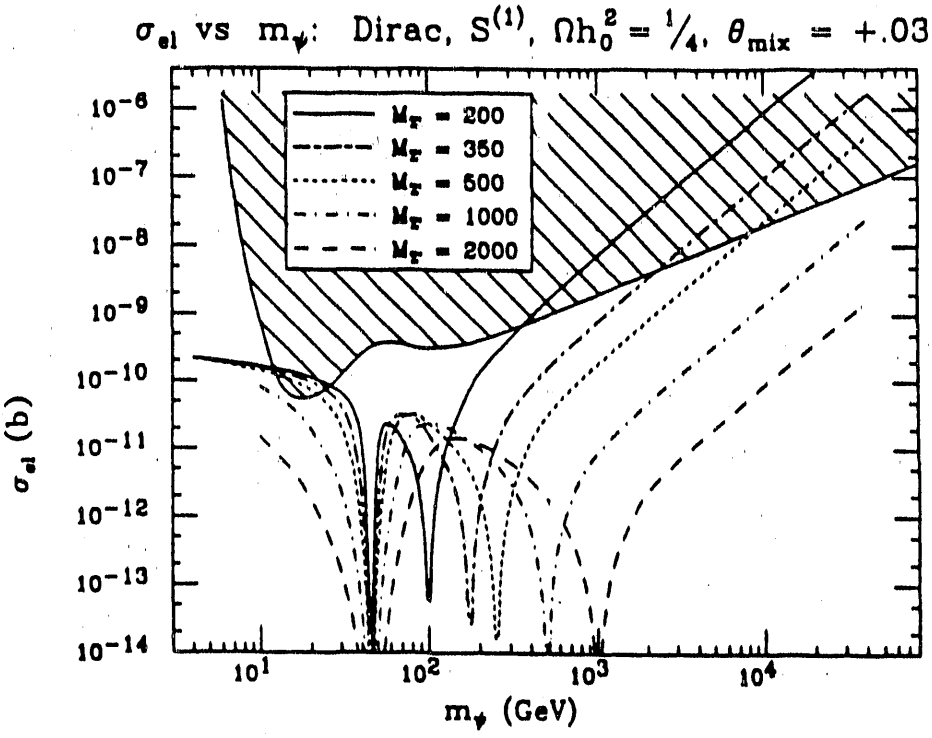

Figure 11: Fig. 6 Modified for $\theta_{mix} = 0.03$

E. FIXED COUPLING g_1'

In Section C.2 we plotted σ_{el} of a Dirac fermion for several fixed values of $M_{Z'}$. Now we will fix the coupling g_1', and let $M_{Z'}$ adjust to satisfy eq. (II.C.18). In particular, we will pay homage to the GUT's by taking $g_1' = 0.46$, as well as exploring a range around that value. We can also use the $M_{Z'}$ limits of eq. (II.D.3), along with eq. (II.C.15), to put lower limits on m_ψ[26]:

$$m_\psi > 55\,\text{GeV}\,(S^{(1)}), \quad m_\psi > 20\,\text{GeV}\,(S^{(2)}), \quad m_\psi > 13\,\text{GeV}\,(S^{(3)}) \qquad \text{(II.E.1)}$$

where each value should be multiplied by $\sqrt{.25/\Omega h_0^2}$.

At fixed g_1' and $M_{Z'}$, eq. (II.C.18) has two solutions for m_ψ, one below $\frac{1}{2}M_{Z'}$ and one above. So as we let $M_{Z'}$ vary, we get two branches (the "low" and "high" branches) in our plot of σ_{el} vs. m_ψ, Fig. 12. The low branch looks similar to Fig. 4 [but with eq. (II.E.1) imposed], since σ_{el} is nearly independent of $M_{Z'}$ for $m_\psi \ll M_{Z'}$. The nearly vertical nature of the high branch can be understood from eq. (II.C.20), which shows that for low Z' masses, $m_\psi = 650\,\text{GeV}$, while from (II.C.21) we know $\sigma_{el} \sim 1/M_{Z'}^4$. Lower limits on $M_{Z'}$ in this case translate to upper limits on σ_{el}.

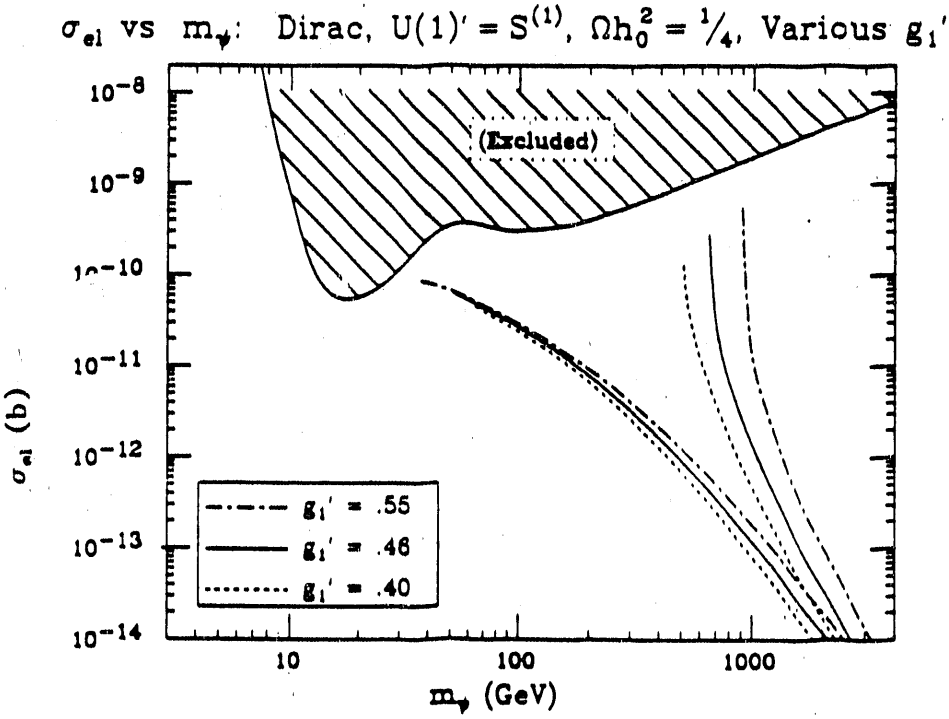

Figure 12: σ_{el} vs. m_ψ: Dirac, $S^{(1)}$, $\Omega h_0^2 = \frac{1}{4}$, Various g_1'

GUT's which fix g_1' restrict σ_{el} and m_ψ to these 2 branches.

In Fig. 13 we have superimposed the GUT-constrained cross-sections ($g_1' = 0.46$) from all seven of our candidate symmetries. We have arbitrarily taken $M_{Z'} > 180\,\text{GeV}$ for symmetries 4–7.

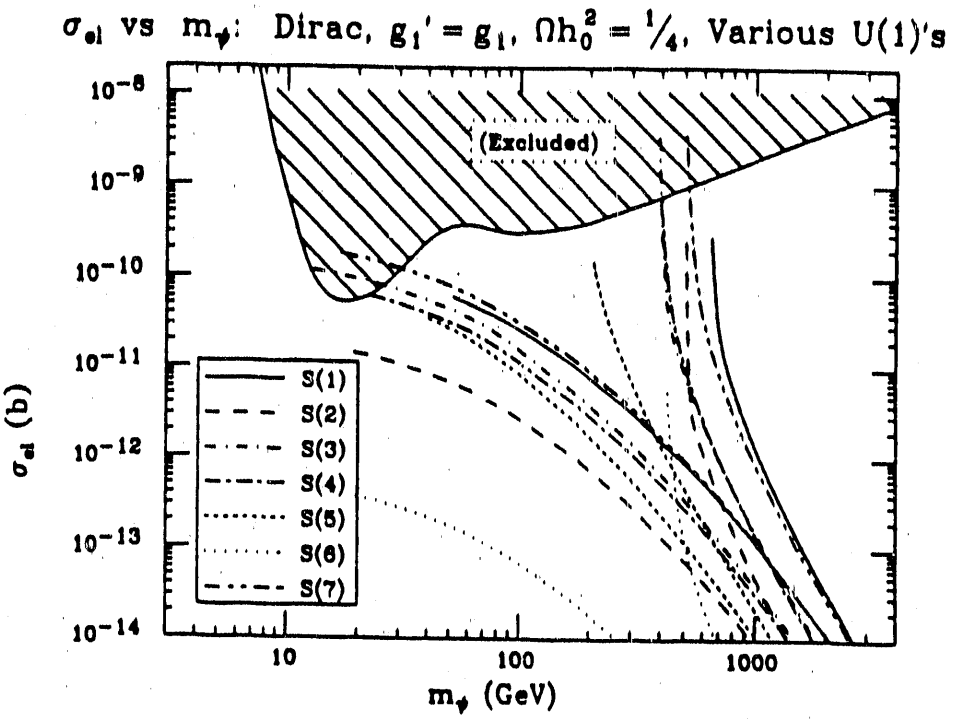

Figure 13: σ_{el} vs. m_ψ: Dirac, $g_1' = g_1 = 0.46$, $\Omega h_0^2 = \frac{1}{4}$, Various U(1)'s, from GUT's with no intermediate mass scale.

F. CONCLUSIONS

As long as $m_\psi \ll M_{Z'}$, we can predict σ_{el} vs. m_ψ for a dark-matter U(1)'-coupled Dirac fermion, without knowing any details about the Z' mass, the coupling g_1', or even the fermion charge V_ψ. Uncertainty in the Hubble parameter and in the form of the low-energy U(1)' introduce small uncertainties in σ_{el}. In this regime, the predicted germanium cross-section is close to experimental limits for $10\,\text{GeV} < m_\psi < 100\,\text{GeV}$. Predicted cross-sections for Majorana fermions are much lower.

Another window of experimental detection opens for $m_\psi > \frac{1}{2}M_{Z'}$, anywhere in the range $400\,\text{GeV} < m_\psi < 40\,\text{TeV}$, but now the predicted cross-section depends on $M_{Z'}$ (or, equivalently, on g_1'). In Fig. 6 we chose to fix $M_{Z'}$, while in Figs. 12 and

13 we fixed g_1' to be the value predicted by certain GUT's. In the latter case, lower limits on $M_{Z'}$ translate to lower limits on m_ψ and upper limits on $\sigma_{\rm el}$.

Under the fairly general assumptions that the dark matter is a U(1)′-coupled fermion, with no particle-antiparticle asymmetry, and with the local density and velocity distribution of the galactic halo, we have shown that dark matter detectors can powerfully probe the U(1)′ sector.

G. APPENDIX: FORMULAS FOR Φ_d, Υ_d, Φ_m, AND Υ_m

Eqs. (II.C.14), (II.C.23), (II.C.29), and (II.C.34) can be calculated for any U(1)′ symmetry from its β, λ, and κ values using

$$\begin{aligned}
\left(\textstyle\sum_f S_f^2\right)(m_\psi < m_t) &= \tfrac{37}{3}\beta^2 + \tfrac{103}{12}\lambda^2 + \tfrac{43}{3}\kappa^2 + \tfrac{43}{3}\beta\lambda - \tfrac{46}{3}\beta\kappa - \tfrac{17}{3}\lambda\kappa \\
\left(\textstyle\sum_f S_f^2\right)(m_\psi > m_t) &= 13\beta^2 + 10\lambda^2 + 16\kappa^2 + 16\beta\lambda - 16\beta\kappa - 8\lambda\kappa \\
V_{\rm Ge}/A &= 2\beta + .94\lambda - \kappa \\
S_Q + S_{D^c} &= \tfrac{1}{2}\lambda + \kappa
\end{aligned} \tag{II.G.1}$$

The terms V_ψ and A_ψ depend on the form of ψ [see eq. (II.C.1)],

$$\begin{aligned}
\psi = \begin{pmatrix} \bar{N} \\ N^c \end{pmatrix} &: V_\psi = \beta - 2\kappa, \qquad \psi = \begin{pmatrix} \bar{N} \\ P \end{pmatrix} : V_\psi = -2\kappa \\
\psi = \begin{pmatrix} \bar{N}^c \\ N^c \end{pmatrix} &: A_\psi = 2\beta, \qquad \psi = \begin{pmatrix} \bar{N} \\ N \end{pmatrix} : A_\psi = 4\kappa
\end{aligned} \tag{II.G.2}$$

III. FLIPPED SU(5) WITH R_P VIOLATION

There are more things in heaven and earth, Horatio, than are dreamt of in your philosophy.

– "Hamlet" (W. Shakespeare)

A. INTRODUCTION AND MOTIVATION

It is often said that the most important experimental signature of supersymmetry is missing energy. In fact, this signature only occurs in those supersymmetric models which are also R_P invariant and have a neutral lightest superpartner (LSP). It has recently been stressed that it is worthwhile searching for supersymmetric signatures in models without R_P invariance[27]; such signatures are exotic and typically easily identified[27–34]. It is trivial to write down R_P-violating $SU(3) \otimes SU(2) \otimes U(1)$ models, even with the minimal field content of Q, U^c, D^c, L, E^c, h and $\bar{h}$. The "$\Delta L \neq 0$" model contains LLE^c, QLD^c, and $\mu L\bar{h}$, while the "$\Delta B \neq 0$" model contains $U^cD^cD^c$ in the superpotential. At the $SU(3) \otimes SU(2) \otimes U(1)$ level there is little reason to choose the usual R_P invariant model (conserving both B and L) over models which violate either B or L. In each model the effective theory at the TeV scale contains a global U(1) symmetry (R_P, B, or L). Clearly, experimental searches should be made for all three. However, this leaves open an important theoretical question: which version is most likely to be the remnant of symmetry breaking at a higher energy scale?

The very simplest unified schemes do tend to give the standard R_P conserving model. For example, R_P can result in SO(10) models from the requirement that all interactions have an even number of spinor representations. In SU(5) theories, LLE^c, QLD^c, and $U^cD^cD^c$ all come from the same operator, which must therefore be absent to avoid proton decay (see Fig. 14). On the other hand, there is absolutely no reason that these simplest of all GUT's are the ones chosen by nature. We find it

interesting that only mild additions are required to obtain an R_P violating low-energy theory. Even in SU(5), lepton number violation can occur at the renormalizable level in the low energy effective theory[33]. This is because Higgs and lepton doublets have the same gauge quantum numbers and can have mass mixing. This case is particularly interesting because the flavor dependence of the lepton number violation is highly constrained. Another unusual possibility is that the extra low-energy global symmetry is a discrete Z_N symmetry ($N > 2$), as might arise from compactification in superstring inspired models[35]. In this case the L or B violation which causes LSP decay occurs via higher dimension operators.

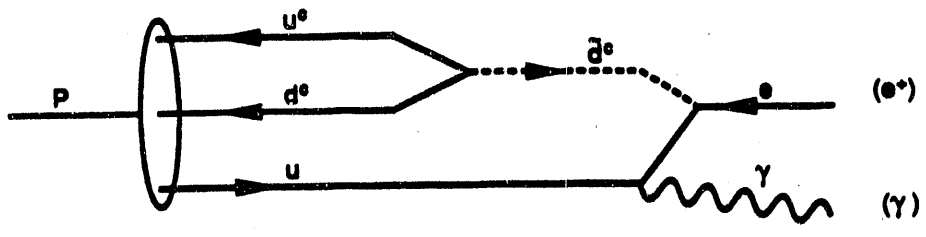

Figure 14: Proton decay from $U^cD^cD^c$ and QLD^c

In this chapter we consider a new way of obtaining the R_P violating "$\Delta L \neq 0$" model. Our model is based on the Flipped SU(5) $\otimes$ U(1) gauge group[11,12] ($\overline{\text{SU(5)}}$ for short), where electric charge is embedded partly in each simple factor. Unlike conventional SU(5)[10], this group allows simple operators which yield LLE^c, without giving $U^cD^cD^c$. In subsequent sections we describe the model and its experimental consequences in some detail. Certainly the model is not perfect: it loses the two good predictions of conventional SU(5), namely $\sin^2\theta_W$[36] and m_b/m_τ[37]; it is not even a true GUT in that the group is not semi-simple. Nevertheless, we find some elegant and unusual features, together with some constrained predictions, which we list here:

- This model has the fewest superfields of any supersymmetric SU(5) model known to us, all in low-dimension representations ($\underline{5}$'s and $\underline{10}$'s).
- Decuplets ($\underline{10}$, $\overline{10}$) of SU(5) break SU(5) $\otimes$ U(1) to SU(3) $\otimes$ SU(2) $\otimes$ U(1) and leave light Higgs doublets in a very elegant missing partners mechanism[12,38].
- The grand unified scale is generated dynamically by renormalization group scaling of supersymmetry breaking scalar masses.
- The Higgs mixing term $mh\bar{h}$, with m at the weak scale, is generated by the same symmetry that suppresses low-energy B violation.
- The incorrect mass relation of conventional SU(5), $m_d/m_s = m_e/m_\mu$, is absent.
- The charged lepton masses do not arise from Yukawa couplings of the unified theory. The μ and τ masses arise from the same higher-dimension operators which are responsible for the L violation, which is therefore highly constrained.
- The electron mass occurs at even higher dimension and is consequently small.
- A seesaw mechanism makes neutrinos light, with ν_τ a candidate for dark matter.
- The electron neutrino has a Majorana mass close to its present limit from neutrinoless double beta decay.
- $Z^0 \to e^-\mu^+e^+\mu^-$, where each (e, μ) pair has invariant mass equal to $m(\tilde{\nu}_\mu)$, occurs with a large branching ratio if $m_{\tilde{\nu}} < M_Z/2$. If sneutrinos are heavier, $Z^0 \to e^-\tau^+e^+\tau^-$ is the dominant signal, but is too rare to be seen at LEP.

To avoid processes like $\mu \to e\gamma$ and $K_L \to \mu e$, we cannot allow strong violation of several lepton family numbers[27]. Of the nine terms $\frac{1}{2}C^{ijk}L_iL_jE_k^c$ (by antisymmetry of the generation indices i and j), each of which violates exactly one or three family numbers, our theory must allow only those that violate a single family number. Our model primarily violates electron number. The strictest limits on our coefficients C^{212} and C^{313} then come from the electron neutrino Majorana mass.

B. A $\overline{SU(5)}$ MODEL WITH ELECTRON-NUMBER VIOLATION

Our model employs a discrete symmetry called η_P (replacing R_P or the $H \to -H$ symmetry of [12]), which has been chosen to allow the operator which contains LLE^c but forbid B violation. Our left-handed chiral superfields have the following SU(5) structure, U(1) charge, and η_P charge:*

$$F_i = (\underline{10}, 1, -1), \quad \bar{f}_i = (\overline{5}, -3, 1), \quad E_i^c = (\underline{1}, 5, -1),$$
$$H = (\underline{10}, 1, 3), \quad \bar{H} = (\overline{10}, -1, 4), \quad h = (\underline{5}, -2, -2), \quad \bar{h} = (\overline{5}, 2, 4) \tag{III.B.1}$$

Here i, j, k are generation indices (1 to 3). The matter multiplets contain:

$$F = \begin{pmatrix} 0 & d_3^c & -d_2^c & d_1 & u_1 \\ & 0 & d_1^c & d_2 & u_2 \\ & & 0 & d_3 & u_3 \\ & & & 0 & \nu^c \\ & & & & 0 \end{pmatrix} \qquad \bar{f} = \begin{pmatrix} u_1^c \\ u_2^c \\ u_3^c \\ \nu \\ e \end{pmatrix} \tag{III.B.2}$$

H and $\bar{H}$ take GUT-scale vev's $\langle H_{45} \rangle = \langle \bar{H}_{45} \rangle = V$ (we will explore the dynamical generation of the GUT scale in Section III), while the remaining fields in H and $\bar{H}$ acquire GUT-scale masses from the missing partners mechanism[12,38] (along with the triplet parts of h and $\bar{h}$) and the Super-Higgs effect. The doublet parts of h and $\bar{h}$ are the low-energy Higgses, taking vev's in the h_5 and $\bar{h}_5$ directions; these become the isospin $+\frac{1}{2}$ piece of the h doublet (hypercharge $-\frac{1}{2}$) and the isospin $-\frac{1}{2}$ piece of the $\bar{h}$ doublet (hypercharge $+\frac{1}{2}$).

Under η_P, $\theta \to i\theta$ and superfields transform as $e^{2\pi i \eta_P/8}$, so for a superpotential term to be invariant the sum of the η_P charges must equal 4 (mod 8). To zeroth

*The η_P charges are just one of a family of equivalent assignments, differing by a multiple of the U(1) charge: $F(x-1)$, $\bar{f}(-3x+1)$, $E^c(5x-1)$, $H(x+3)$, $\bar{H}(-x+4)$, $h(-2x-2)$, $\bar{h}(2x+4)$, all mod(8).

order in $1/M_P$ our superpotential is simply:

$$W^{(0)} = \lambda_1^{ij} F_i F_j h + \lambda_2^{ij} F_i \bar{f}_j \bar{h} + \lambda_4 HHh + \lambda_5 \bar{H}\bar{H}\bar{h} \qquad \text{(III.B.3)}$$

This generates down quark masses, up quark masses, and the missing partners mechanism.

The lepton-number violating term arises at first order in $\epsilon \equiv (M_G/M_P)$ (where M_G is the GUT scale):

$$W^{(1)} = \lambda_A M_P^{-1} H \bar{f} \bar{f} E^c \rightarrow \tfrac{1}{2} \bar{C}^{ijk} L_i L_j E_k^c \qquad \text{(III.B.4)}$$

as H takes its vev, so we expect $\bar{C}^{ijk} \leq \epsilon$. In formulating η_P, we saw immediately that no symmetry could allow down masses (FFh), charged lepton masses ($h\bar{f}E^c$), and the L-violating term of (III.B.4) ($H\bar{f}\bar{f}E^c$), without also allowing the B- and L-violating term $HFF\bar{f}$. We could have chosen to retain $h\bar{f}E^c$ but not $H\bar{f}\bar{f}E^c$, violating L through a term $(H\bar{H})^n H\bar{f}\bar{h} \rightarrow \mu L\bar{h}$. Then a rotation of L and h would generate $\frac{1}{2}C^{ijk}LLE^c$ with C^{313} and/or C^{323} dominant, as in Hall and Suzuki's SU(5) model[33]. Instead, we chose (by our choice of η_P) to disallow the $h\bar{f}E^c$ term and generate lepton masses (for μ and τ only!) from $H\bar{f}\bar{f}E^c$, by the rotation of L_1 and h.

This rotation is due to the superpotential terms

$$\begin{aligned} W^{(2)} &= \lambda_B M_P^{-8} (H\bar{H})^4 H\bar{f}\bar{h} + \lambda_C M_P^{-11} (H\bar{H})^6 h\bar{h} \\ &\rightarrow \mu^i L_i \bar{h} + m h\bar{h} \qquad (\mu^i = \epsilon^9 \lambda_B M_P, \quad m = \epsilon^{12} \lambda_C M_P) \end{aligned} \qquad \text{(III.B.5)}$$

The combination of fields which couples to $\bar{h}$ will be the one we call the low-energy Higgs; this coupling is responsible for breaking PQ-symmetry and allowing both Higgses to take vev's[39], so that our theory correctly breaks $SU(2)_L \otimes U(1)_Y \rightarrow U(1)_{EM}$. Let us first rotate the L_i (which are still degenerate, being massless) so that the linear combination of these which couples to $\bar{h}$ is now called L_1, then rotate

this L_1 with h such that the linear combination which couples with $\bar{h}$ is now called h':

$$h' = c_1 h + s_1 L_1, \quad L_1' = c_1 L_1 - s_1 h, \quad L_2' = L_2, \quad L_3' = L_3 \tag{III.B.6}$$

The rotation angle is given by $s_1/c_1 = \mu/m$.

The lepton mass matrix is now generated from equation (III.B.4):

$$W^{(1)} \to s_1 \bar{C}^{i1k} L_i' h' E_k^c + c_1 \bar{C}^{i1k} L_i' L_1' E_k^c + \bar{C}^{23k} L_2' L_3' E_k^c \tag{III.B.7}$$

Since $\bar{C}^{ijk}$ is antisymmetric in (i, j), the first term gives masses to the muon and tau only, smaller than the quark masses by $\mathcal{O}(\epsilon)$, while the electron remains massless. A term

$$W^{(3)} = \lambda_E M_P^{-4} (H\bar{H})^2 \bar{f} E^c h \tag{III.B.8}$$

gives a small electron mass of $\epsilon^4 \langle h' \rangle$; we will find from M_W/M_P that $\epsilon = .04$ in our model, so $m_e \approx$ MeV. The electron is light because it is the combination of L_i that rotated with h! The second and third terms of $W^{(1)}$ violate lepton number as desired. The rotation also affects the down quark mass term,

$$\lambda_1^{ij} Q_i h D_j^c \to c_1 \lambda_1^{ij} Q_i h' D_j^c - s_1 \lambda_1^{ij} Q_i L_1' D_j^c \tag{III.B.9}$$

The second term is electron-number violating, diagonal in the quark flavors and dominated by the third quark generation: $D^{313} Q_3 L_1 D_3^c$. From (III.B.7) and (III.B.9) we see:

$$C^{212} = \frac{c_1 m_\mu}{s_1 \langle h' \rangle}, \quad C^{313} = \frac{c_1 m_\tau}{s_1 \langle h' \rangle},$$

$$D^{111} = \frac{-s_1 m_d}{c_1 \langle h' \rangle}, \quad D^{212} = \frac{-s_1 m_s}{c_1 \langle h' \rangle}, \quad D^{313} = \frac{-s_1 m_b}{c_1 \langle h' \rangle} \tag{III.B.10}$$

With the diagonalization of the lepton and quark mass matrices, all other lepton-number violating coefficients vanish except for the three terms C^{23k}, which must be taken small by fiat. Our theory violates only electron number.

The electron neutrino Majorana mass diagrams of Fig. 15 constrain the rotation angle. Too much rotation ($\mu \gg m$) makes D^{313} large and Figure 15a dominates, with

$$m_M(\nu_e) = \frac{3A_b}{16\pi^2}\left(\frac{s_1}{c_1}\right)^2 \frac{m_b^4 M_{3/2}}{\langle h'\rangle^2 m_{\tilde{b}^c}^2} < 2\,\mathrm{eV} \qquad \text{(III.B.11a)}$$

where the limit is obtained from neutrinoless double-beta decay experiments. Too little rotation ($\mu \leq m$) makes C^{313} large and Figure 15b dominates, with

$$m_M(\nu_e) = \frac{A_\tau}{16\pi^2}\left(\frac{c_1}{s_1}\right)^2 \frac{m_\tau^4 M_{3/2}}{\langle h'\rangle^2 m_{\tilde{\tau}}^2} < 2\,\mathrm{eV} \qquad \text{(III.B.11b)}$$

Reconciling (III.B.11a) and (III.B.11b) forces us to make the rotation angle about 20° and the A parameters (renormalized down to $M_{3/2}$) small, about 1/10. Small values for the A's are plausible from the renormalization equations if $A \approx -4M_0$ at the Planck scale; equation (A.11) of reference [39] predicts $A_b, A_\tau(M_{3/2}) = A + 4M_0$ (another possibility is to take A_b and A_τ of opposite sign, so (III.B.11a) and (III.B.11b) tend to cancel). With[39]

$$M_{3/2} = 1\ \mathrm{TeV},\ \langle h'\rangle = 130\ \mathrm{GeV},\ m_{\tilde{b}^c}^2 = 7.6\,M_{3/2}^2,\ m_{\tilde{\tau}}^2 = 1.5\,M_{3/2}^2 \qquad \text{(III.B.12)}$$

we calculate a barely acceptable mass for $A \approx .1$ and $s_1 \approx .38$. This allows us to predict (in the sense that the given values require the least fine-tuning of A) the C^{ijk}'s and D^{ijk}'s from (III.B.10).

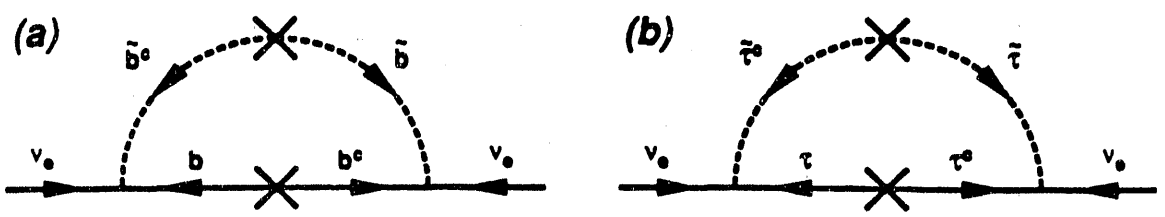

Figure 15: Radiative Corrections to Electron Neutrino Mass

To achieve this rotation angle, we must make $\lambda_B/\lambda_C = 2 \times 10^{-4}$. Then to get the weak scale right in equation (III.B.5) (with $\lambda_C \approx \mathcal{O}(1)$), we find $\epsilon = .04$.

The neutrino seesaw mechanism is driven by the term

$$W^{(4)} = \lambda_N M_P^{-5} (H\bar{H})^2 (F\bar{H})^2 \qquad \text{(III.B.13)}$$

ν^c gets a Majorana mass of order $\epsilon^6 M_P \approx 4 \times 10^{10}\,\text{GeV}$; then the λ_2 term couples ν^c to ν, giving ν a seesaw mass:

$$m_{\nu_L} \approx \frac{m_u^2}{4 \times 10^{10}\,\text{GeV}} = 3 \times 10^{-6}\,\text{eV (e)}, \quad .1\,\text{eV}\ (\mu), \quad 100\,\text{eV}\ (\tau) \qquad \text{(III.B.14)}$$

with $m_t = 70\,\text{GeV}$. The ν_τ is cosmologically stable and is a constituent of the dark matter.

Undesirable superpotential terms are neatly suppressed by η_P:

$$W^{(5)} = \lambda_F M_P^{-13} (H\bar{H})^6 HFF\bar{f} + \lambda_G M_P^{-13} (H\bar{H})^7 F\bar{H} + \lambda_H M_P^{-5} (H\bar{H})^4 \qquad \text{(III.B.15)}$$

The first violates B and L, while the second and third threaten the flatness of the $H = \bar{H} = V$ direction. Actually, we need $\lambda_H \leq 10^{-4}$ to avoid this pitfall. Other highly-suppressed or unimportant terms are collected for completeness's sake in $W^{(6)}$:

$$\begin{aligned} W^{(6)} = {} & M_P^{-3} (H\bar{H}) \bar{H}\bar{h}\bar{f} + M_P^{-5} (H\bar{H})^2 HHF\bar{f} + M_P^{-8} (H\bar{H})^4 HFh \\ & + M_P^{-12} (H\bar{H})^5 \bar{H}\bar{H}\bar{H}hE^c + M_P^{-13} (H\bar{H})^6 HHH\bar{f} \end{aligned} \qquad \text{(III.B.16)}$$

We do not have exact mass relation predictions, but up to Yukawa couplings we expect:

$$m(\mu)/m(c) \approx m(\tau)/m(t) \approx \epsilon = .04 \text{ (experimentally } \approx .08, .03) \qquad \text{(III.B.17)}$$

$$m(s)/m(c) \approx m(b)/m(t) \approx c_1 = .9 \text{ (experimentally } \approx .15, .07) \qquad \text{(III.B.18)}$$

$$m(e) \approx \epsilon^4 \langle h' \rangle \approx \text{MeV (experimentally } = 511\,\text{keV}) \qquad \text{(III.B.19)}$$

Other numerical predictions of our model are:

$$M_G/M_P = .04 \tag{III.B.20}$$

$$m(\nu) \approx 2\,\text{eV (e)}, \quad .1\,\text{eV}\ (\mu), \quad 100\,\text{eV}\ (\tau) \tag{III.B.21}$$

$$C^{212} = .002, \quad C^{313} = .034, \quad D^{212} = -.0006 \quad D^{313} = -.015 \tag{III.B.22}$$

with other C^{ijk}'s and D^{ijk}'s small or zero. Note the largest C^{ijk} is indeed $\mathcal{O}(\epsilon)$, as expected.

C. RENORMALIZATION SCALING BEHAVIOR

In this section we will find $g_1 = g_5$ at M_G; we will derive the gaugino mass relation necessary for our model to break down correctly to the Standard Model, and we will explore the origin of the GUT scale.

g_1 is the coupling constant associated with the normalized U(1) charge $q = \sqrt{\frac{1}{40}}Q$, Q being the charge given in equation (III.B.1). From renormalization scaling of known low-energy couplings,[40] $g_5(M_G) = .724$ (from α_3 and α_2) and $g_y(M_G) = .703$ ($y = \sqrt{\frac{3}{5}}Y$, and taking $\sin^2\theta_W = .228$). Since we know

$$y = \sqrt{\frac{24}{25}}\,q + \sqrt{\frac{1}{25}}\,T_{24} \tag{III.C.1}$$

we can define an angle θ_X analogous to the Weinberg angle:

$$g_y = g_1\sqrt{\frac{25}{24}}\cos\theta_X = g_5\sqrt{25}\sin\theta_X, \qquad \tan\theta_X = \sqrt{\frac{1}{24}}\,\frac{g_1}{g_5} \tag{III.C.2}$$

The known values give us $\sin^2\theta_X = .0377$ and $g_1/g_5 = .97$ at M_G. An SO(10) embedding would predict $\sin^2\theta_X = .04$ and $g_1/g_5 = 1$. Without committing to SO(10), we will hereafter take $g_1 = g_5 \equiv g$.

We must be sure the vacuum breaks correctly, since there are three flat directions in our model: $\langle H\rangle = \langle \bar{H}\rangle = V$, $\langle F_i\rangle = \langle \bar{H}\rangle = \hat{V}$ (for one value of i), and $\langle h\rangle = \langle \bar{h}\rangle = v$. The direction chosen by the theory to break the $\overline{\mathrm{SU}(5)}$ symmetry and define the GUT scale depends on the renormalization behavior of the scalar masses. The Supergravity SUSY-breaking Lagrangian is[41]:

$$\mathcal{L}_{SX} = -m_A^2|A_i|^2 - [AW_3(A_i) + BW_2(A_i) + h.c.] - [\tfrac{1}{2}M_0\lambda^a\lambda^a + h.c.] \qquad \text{(III.C.3)}$$

We take all scalar masses m_A equal, all trilinear soft breaking coefficients A equal, all bilinear coefficients B equal, and all gaugino masses M_0 equal, all $\mathcal{O}(M_{3/2})$, at M_P. We must ask which sum goes negative first as we go down in energy: $(m_H^2 + m_H^2)$, $(m_F^2+m_H^2)$, or $(m_h^2+m_h^2)$. It is easy to make m_F^2 scale less quickly than m_H^2 by making λ_1 and λ_2 small compared to λ_4. Making the h masses scale more slowly than the H masses is more difficult. It turns out that the HHh term contributes equally to the renormalization scaling of m_h^2 and m_H^2, so the correct breaking depends on gaugino masses only. We start with reference [42], equations (A.20–23), then eliminate all terms involving ϕ, λ_1, or λ_2; set $\lambda_4 = \lambda_5 \equiv \lambda$; and define $\hat{m}_H^2 \equiv (m_H^2 + m_H^2)/2$, etc.; to get:

$$\frac{d}{dt}(\hat{m}_H^2) = \frac{1}{16\pi^2}\left[6\lambda^2(2\hat{m}_H^2 + \hat{m}_h^2 + \hat{A}^2) - \frac{g^2}{5}(144M_5^2 + M_1^2)\right] \qquad \text{(III.C.4a)}$$

$$\frac{d}{dt}(\hat{m}_h^2) = \frac{1}{16\pi^2}\left[6\lambda^2(2\hat{m}_H^2 + \hat{m}_h^2 + \hat{A}^2) - \frac{g^2}{5}(96M_5^2 + 4M_1^2)\right] \qquad \text{(III.C.4b)}$$

To have the right-hand side of (III.C.4a) greater than that of (III.C.4b), we must have at M_G:

$$M_1(M_G) \geq 4M_5(M_G) \qquad \text{(III.C.5)}$$

discouraging any thoughts of a nearby superunification into SO(10). For a comparable analysis in the $\overline{\mathrm{SU}(5)}$ model of Antoniadis *et al.*, see [40].

Equation (III.C.4a) determines the GUT scale, from

$$\hat{m}_H^2(t=0) = m_A^2\,, \qquad \hat{m}_H^2(t=\ln\epsilon) = 0 \tag{III.C.6}$$

Let

$$\alpha = \frac{18\lambda^2}{16\pi^2}, \quad \beta = \frac{6\lambda^2 A^2}{16\pi^2} - \frac{29 g^2 M_0^2}{16\pi^2} \tag{III.C.7}$$

Then with $\hat{m}_h^2 \approx \hat{m}_H^2$ and (from reference [42], (A.11–12)) $\hat{A} = Ae^{\alpha t}$, but ignoring scaling of g and λ, the solution is

$$\epsilon = \left(1 - \frac{\alpha m_A^2}{\beta}\right)^{1/\alpha} \tag{III.C.8}$$

For $\epsilon = .04$, one choice of parameters obeying (III.C.8) is:

$$g = .724, \quad \lambda = .86, \quad m_A = M_0, \quad A = -4\,M_0 \tag{III.C.9}$$

We have taken $g = .724$ as calculated at the beginning of this section, and $A = -4M_0$ (at M_P) as discussed following equation (III.B.11b). M_0 is undetermined.

D. SIGNATURES OF LEPTON VIOLATION IN RARE Z^0 DECAYS

The signatures of a model violating I differ greatly from the missing-energy signatures of R_p-invariant models. Superpartners can be pair-produced, as in the e^+e^- collisions of Fig. 16, and will decay into ordinary matter through processes such as those in Fig. 17. 1-loop diagrams such as those in Fig. 18 show how a Z^0 could produce a single superpartner and one ordinary particle of fixed energy, a truly spectacular decay which unfortunately has too small a branching ratio to be seen at LEP. Prominent Bhabha scattering resonances occur at the $\tilde{\nu}_\mu$ and $\tilde{\nu}_\tau$ masses, as seen in Fig. 19; though note these interactions are absent in our model (They do occur in the "μ" version of our model; see the Appendix). These signatures are discussed further in references [27–34].

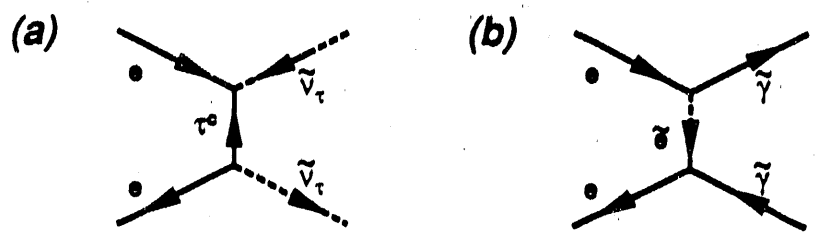

Figure 16: t-Channel Exchange Diagrams

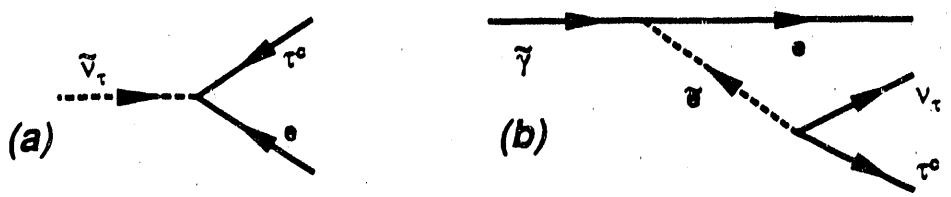

Figure 17: a) Sneutrino Decay, b) Photino Decay

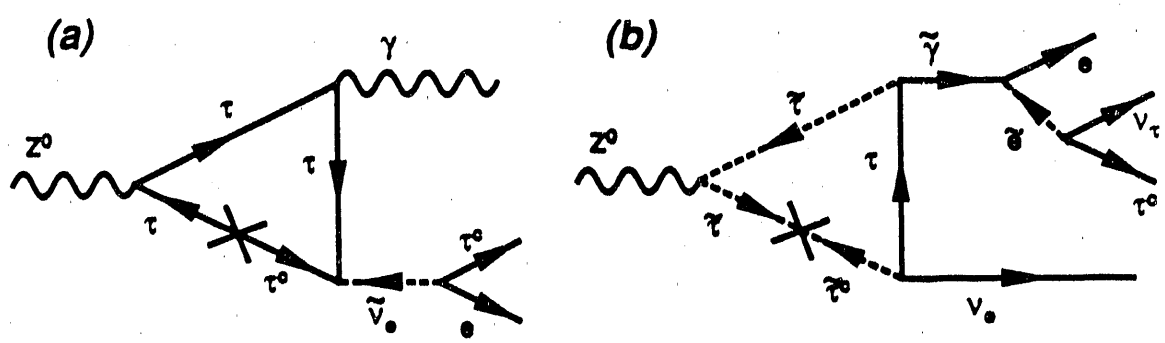

Figure 18: a) $Z^0 \rightarrow \gamma \tilde{\bar{\nu}}_e$, b) $Z^0 \rightarrow \bar{\nu}_\tau \tilde{\gamma}$

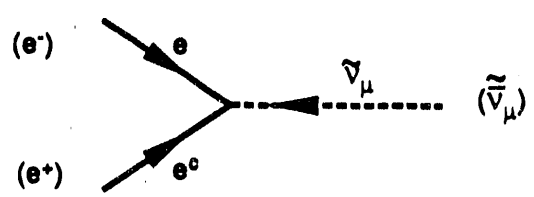

Figure 19: Sneutrino Resonance in the "μ" Version

We will concentrate on rare Z^0 decays which occur in our model with branching ratios of 10^{-6} or larger, so as to be seen at LEP. From equation (III.B.22), we see our largest L-violating coefficient is $C^{313} = .034$, which provides the interactions of Fig. 20.

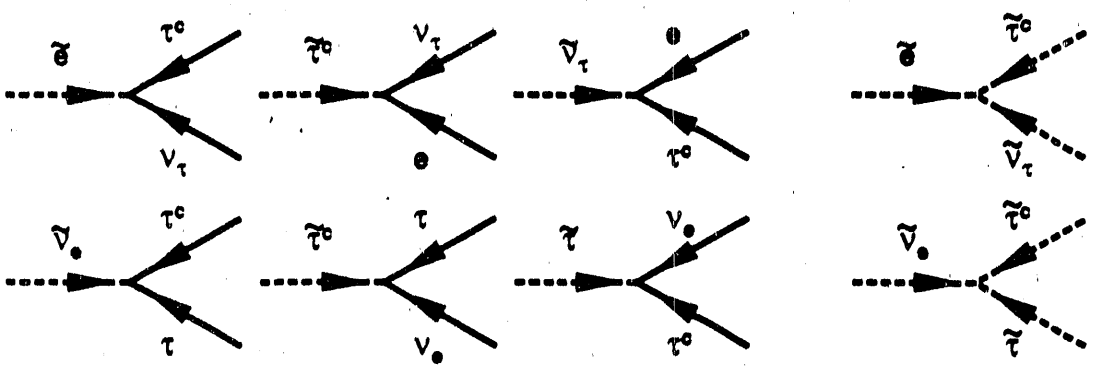

Figure 20: R_P-violating Interactions from C^{313}

Our model predicts the decay $Z^0 \to e^-\tau^+e^+\tau^-$, through the three diagrams of Fig. 21. If $m(\tilde{\nu}) < M_Z/2$, this process proceeds primarily through the production of two on-shell $\tilde{\nu}_\tau$'s (Figure 21a), and the branching ratio is large ($> 10^{-4}$). In this case, the $(e^-\tau^+)$ pair and the $(e^+\tau^-)$ pair would each have an invariant mass equal to the $\tilde{\nu}_\tau$ mass. In fact, sneutrino pair production would lead to equally large branching ratios for all three of these reactions:

$$\begin{aligned} Z^0 &\to e^-\tau^+e^+\tau^-, \quad \sqrt{s_{e^-\tau^+}} = \sqrt{s_{e^+\tau^-}} = m(\tilde{\nu}_\tau) \\ Z^0 &\to e^-\mu^+e^+\mu^-, \quad \sqrt{s_{e^-\mu^+}} = \sqrt{s_{e^+\mu^-}} = m(\tilde{\nu}_\mu) \\ Z^0 &\to \tau^-\tau^+\tau^+\tau^-, \quad \sqrt{s_{\tau^-\tau^+}} = \sqrt{s_{\tau^+\tau^-}} = m(\tilde{\nu}_e) \end{aligned} \tag{III.D.1}$$

If $m(\tilde{\nu}) \geq M_Z/2$, all three diagrams of Figure 21 contribute to $Z^0 \to e^-\tau^+e^+\tau^-$, with 21b and 21c dominating at higher sneutrino masses. In this case only one $(e\tau)$

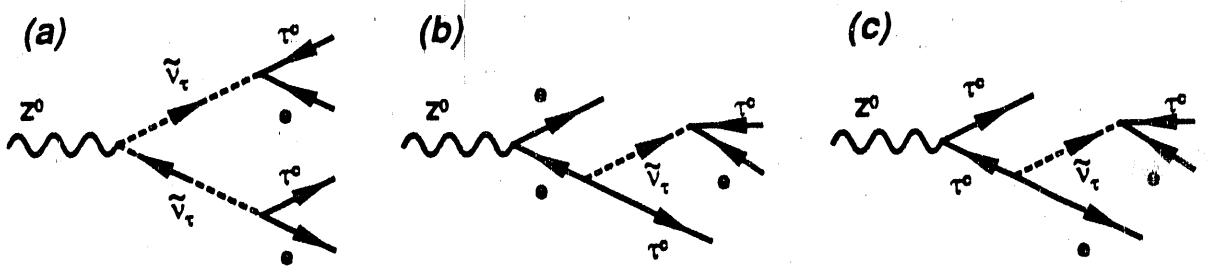

Figure 21: $Z^0 \rightarrow e^-\tau^+e^+\tau^-$

pair comes out with invariant mass equal to $m(\tilde{\nu}_\tau)$. Similar diagrams lead to:

$$\begin{aligned}
Z^0 &\rightarrow e^-\tau^+e^+\tau^- \quad \propto (C^{313})^2 \\
Z^0 &\rightarrow e^-\mu^+e^+\mu^- \quad \propto (C^{212})^2 \\
Z^0 &\rightarrow \tau^-\tau^+\tau^+\tau^- \quad \propto (C^{313})^2 \\
Z^0 &\rightarrow \mu^-\mu^+\tau^-\tau^+ \quad \propto (C^{212})^2 \\
Z^0 &\rightarrow b\bar{b}\tau^-\tau^+ \quad \propto (D^{313})^2 \\
Z^0 &\rightarrow e^-\bar{b}e^+b \quad \propto (D^{313})^2
\end{aligned} \tag{III.D.2}$$

Figure 22 shows total calculated branching ratios for $Z^0 \rightarrow e^-\tau^+e^+\tau^-$ (solid line), plotted against $m(\tilde{\nu}_\tau)$, for $C^{313} = 1.$ (a), and for $C^{313} = .034$ (b) as in our model. The dashed line shows the contribution from Figure 21a; the dotdashed line is from diagrams b and c (and the interference between them); and the dotted line is from interference between a and (b and c). For $C^{313} = .034$, we see that a signal would only be seen at LEP if $m(\tilde{\nu}) < M_Z/2$, but for $C^{313} = 1.$ a signal would be seen for sneutrinos as heavy as 70 GeV.

E. CONCLUSIONS

Our model shows how L-violation can occur in a supersymmetric GUT model, and how rotation of one lepton family with the Higgs singles out that family to

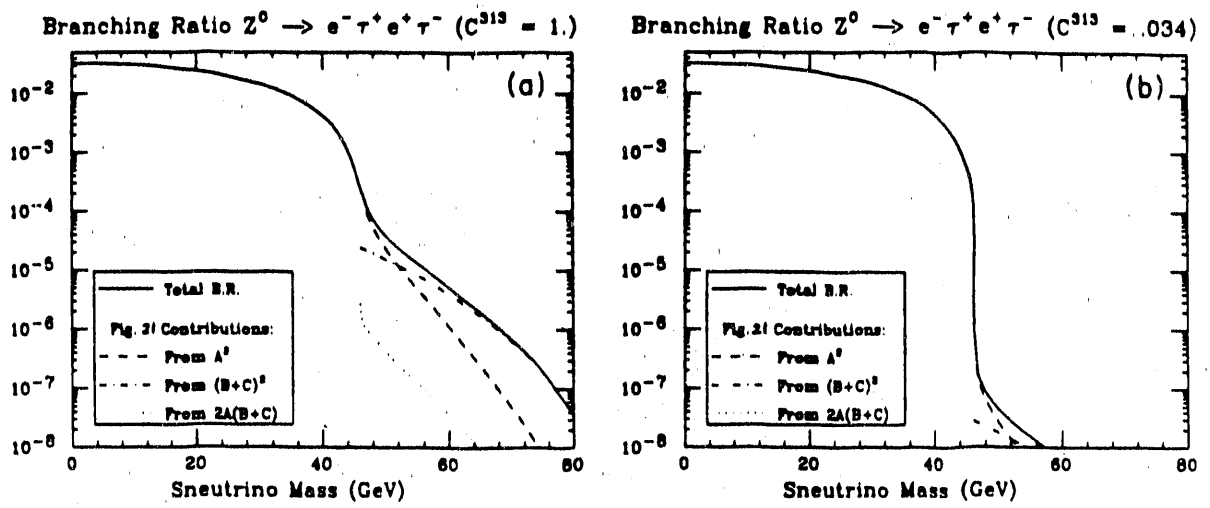

Figure 22: Branching ratios for a) $C^{313} = 1.$, b) $C^{313} = .034$

be light and violated. Since the electron is light, we conclude electron number is violated. The rotation angle is constrained from both sides by limits on the electron neutrino Majorana mass, so from the lepton and quark masses we can predict our largest L-violating terms are $C^{313}L_3L_1E_3^c$ ($C^{313} = .034$), $C^{212}L_2L_1E_2^c$ ($C^{212} = .002$), and $D^{313}Q_3L_1D_3^c$ ($D^{313} = -.015$). We can then calculate branching ratios for Z^0 decays which depend only on the unknown sneutrino masses. If $m(\tilde{\nu}) < M_Z/2$, the clearest signal would come from $Z^0 \to e^-\mu^+e^+\mu^-$, where each (e, μ) pair has invariant mass equal to $m(\tilde{\nu}_\mu)$. If $m(\tilde{\nu}) > M_Z/2$, then branching ratios are proportional to $(C^{ijk})^2$ (or $(D^{ijk})^2$), so for our model $Z^0 \to e^-\tau^+e^+\tau^-$ dominates, though with $C^{313} = .034$ this branching ratio is still rather small. These rare Z^0 decays replace the usual missing-energy signatures, since the LSP is unstable.

F. APPENDIX: A "μ" VERSION OF OUR MODEL

To avoid the neutrino mass constraint, a second version of our model makes the rotated lepton be the muon instead. Now our left-handed chiral superfields have

the following SU(5) structure, U(1) charge, and ζ_P charge:

$$\begin{aligned} &F_i = (\underline{10}\,,1,2), \qquad \bar{f}_i = (\overline{5}\,,-3,-2), \quad E_i^c = (\underline{1}\,,5,2), \\ &H = (\underline{10}\,,1,-7), \quad \bar{H} = (\overline{10}\,,-1,0), \qquad h = (\underline{5}\,,-2,5), \quad \bar{h} = (\overline{5}\,,2,9) \end{aligned} \tag{III.F.1}$$

Superfields transform as $e^{2\pi i\zeta_P/18}$, so the sum of the ζ_P charges in an allowed term must equal 9 (mod 18). The same mechanisms occur as in the η_P model; only the numbers are different, and the rotated lepton superfield is L_2. Our superpotential is:

$$W^{(0)} = \lambda_1^{ij} F_i F_j h + \lambda_2^{ij} F_i \bar{f}_j \bar{h} + \lambda_4 HHh + \lambda_5 \bar{H}\bar{H}\bar{h} \tag{III.F.2}$$

$$W^{(2)} = \lambda_A M_P^{-1} H \bar{f} \bar{f} E^c \to \tfrac{1}{2} C^{ijk} L_i L_j E_k^c \tag{III.F.3}$$

$$W^{(3)} = \lambda_B M_P^{-18} (H\bar{H})^9 H \bar{f} \bar{h} + \lambda_C M_P^{-21} (H\bar{H})^{11} h \bar{h} \tag{III.F.4}$$

$$W^{(3)} = \lambda_E M_P^{-4} (H\bar{H})^2 \bar{f} E^c h \tag{III.F.5}$$

$$W^{(4)} = \lambda_N M_P^{-15} (H\bar{H})^7 (F\bar{H})^2 \tag{III.F.6}$$

$$W^{(5)} = \lambda_F M_P^{-33} (H\bar{H})^{16} HFF\bar{f} + \lambda_G M_P^{-33} (H\bar{H})^{17} F\bar{H} + \lambda_H M_P^{-15} (H\bar{H})^9 \tag{III.F.7}$$

$$\begin{aligned} W^{(6)} = {} & M_P^{-3} (H\bar{H}) \bar{H}\bar{h}\bar{h}\bar{f} + M_P^{-15} (H\bar{H})^7 HHF\bar{f} + M_P^{-18} (H\bar{H})^9 HFh \\ & + M_P^{-22} (H\bar{H})^{10} \bar{H}\bar{H}\bar{H}hE^c + M_P^{-33} (H\bar{H})^{16} HHH\bar{f} \end{aligned} \tag{III.F.8}$$

By setting $m = 50\,\text{GeV}$ (with $\lambda_C = .5$) and $\mu = 1\,\text{TeV}$ (with $\lambda_B = .04$), we get $\epsilon = .17$ and $c_2 = .05$. The ν^c gets a Majorana mass of order $\epsilon^{16} M_P \approx 5 \times 10^6\,\text{GeV}$, so that neutrino masses become .02 eV (e), 700 eV (μ), 500 keV (τ). When L_2 rotates with h, the muon neutrino picks up a mass from the diagrams of Figure 15, but experimental limits on the ν_μ mass are much more forgiving.

Combining the lepton mass and LLE^c terms (see eqs. (III.B.7) and (III.B.8)) now gives (with $i \neq 2$):

$$\begin{aligned} W^{(1)} + W^{(3)} \rightarrow & \lambda^{2k}\langle h'\rangle E'_2 E^c_k + (\mathrm{c}_2\lambda^{ik} + \mathrm{s}_2 C^{i2k})\langle h'\rangle E'_i E^c_k \\ & + C^{13k} L'_1 L'_3 E^c_k + (\mathrm{c}_2 C^{i2k} - \mathrm{s}_2\lambda^{ik}) L'_i L'_2 E^c_k \end{aligned} \tag{III.F.9}$$

Here $\lambda \equiv \epsilon^4 \lambda_E$. A rotation is assumed to diagonalize the mass matrices. The muon mass is $\epsilon^4\langle h'\rangle \approx 100\,\mathrm{MeV}$. The tau (and electron!) masses are smaller than the quark masses by $\mathcal{O}(\epsilon)$. Six of the lepton-number violating terms are suppressed (since c_2 and λ are both small). The Yukawa couplings must conspire to make only one of the three remaining C^{13k} large, and only one of the two remaining charged lepton masses (e, τ) large. From equation (III.B.10), we see that in the quark sector we have a large $Q_3 L_2 D^c_3$ term, with $D^{323} = -.72$.

Up to Yukawa couplings we expect:

$$m(e)/m(u) = m(\tau)/m(t) = \epsilon = .17 \text{ (experimentally } \approx .09,\ .03) \tag{III.F.10}$$

$$m(s)/m(c) = m(b)/m(t) = \mathrm{c}_2 = .05 \text{ (experimentally } \approx .15,\ .07) \tag{III.F.11}$$

$$m(\mu) = \epsilon^4\langle h'\rangle = 100\,\mathrm{MeV} \text{ (experimentally } = 106\,\mathrm{MeV}) \tag{III.F.12}$$

$$m(\nu) = .02\,\mathrm{eV}\ (\mathrm{e}),\quad 700\,\mathrm{eV}\ (\mu),\quad 500\,\mathrm{keV}\ (\tau) \tag{III.F.13}$$

This model has the advantage that it explains why down-type heavy quarks are lighter than their up-type partners (by c_2), and it avoids the strict mass limits on ν_e. Muon number (rather than electron number) is violated. $\tilde{\nu}_\mu$'s would be produced copiously at e^+e^- colliders through the diagram of Figure 19. However, this model fails to explain the lightness of the electron.

IV. RARE Z^0 DECAYS FROM R_P VIOLATION

All great truths begin as blasphemies.
– "Anajanska" (George Bernard Shaw)

A. INTRODUCTION

We showed in the previous chapter that viable models can be built which do not conserve R_P, though one needs some symmetry (such as L or B separately) to avoid fast proton decay. R_P may be broken spontaneously or explicitly; in either case a sneutrino vev often results.

A sneutrino vev causes mixing of the neutrino and zino, which gives neutrinos a mass. Thus, the ν_τ mass limit of 35 MeV restricts $v_\tau \lesssim 5\,\mathrm{GeV}$ over most of SUSY parameter space. The sneutrino vev also mixes charged leptons with winos. Since the gauge eigenstates being mixed have different couplings to the Z^0, the Z^0 couplings to the mass eigenstates are not diagonal, and decays such as $Z^0 \to \bar{\nu}_\tau \chi^0$ and $Z^0 \to \tau^+ \chi^-$ occur. Here χ^0, χ^- are the lightest neutralino and chargino, respectively.

Most models violating R_P explicitly start with the term Lh_2 (h_2 is the Higgs responsible for up masses), and eliminate it by rotating the superfields L and h_1. The resulting superpotential term QD^cL allows χ^0 and χ^- to decay to b-jets and a lepton. Models with spontaneous R_P-breaking also allow χ^0 and χ^- to decay, though with less distinctive signatures.

We calculate the branching ratios for these Z^0 decays to be as large as 3×10^{-5} if m_ν is at its experimental limit, and supersymmetry parameters are favorable. If χ^0 and χ^- are heavier than 45 GeV, this may be the best way to detect them at LEP I.

B. FERMION MASS MIXING

In the presence of a sneutrino vev, the neutral fermion mass matrix is:

$$(\tilde{B}\ \tilde{W}^3\ \tilde{h}_1^0\ \tilde{h}_2^0\ \nu)\begin{pmatrix} bM & 0 & -\frac{1}{2}g'v_1 & \frac{1}{2}g'v_2 & -\frac{1}{2}g'v_\tau \\ 0 & M & \frac{1}{2}gv_1 & -\frac{1}{2}gv_2 & \frac{1}{2}gv_\tau \\ -\frac{1}{2}g'v_1 & \frac{1}{2}gv_1 & 0 & -\mu & 0 \\ \frac{1}{2}g'v_2 & -\frac{1}{2}gv_2 & -\mu & 0 & 0 \\ -\frac{1}{2}g'v_\tau & \frac{1}{2}gv_\tau & 0 & 0 & 0 \end{pmatrix}\begin{pmatrix} \tilde{B} \\ \tilde{W}^3 \\ \tilde{h}_1^0 \\ \tilde{h}_2^0 \\ \nu \end{pmatrix} \qquad \text{(IV.B.1)}$$

Here $\langle h_1^0\rangle = v_1/\sqrt{2}$, $\langle h_2^0\rangle = v_2/\sqrt{2}$, and $\langle \nu_\tau\rangle = v_\tau/\sqrt{2}$. We will assume gaugino masses scale as gauge couplings, $b = 5\alpha_1/3\alpha_2 = 0.49$.

For given $(\mu,\ M)$ and v_1/v_2 we can diagonalize (IV.B.1) to find the masses m_i and eigenvectors $\mathbf{q}_i$ for the five neutralinos χ_i^0 (with $\chi_5^0 = \nu_\tau$). We fix v_τ by setting $m_5 = 35\,\mathrm{MeV}$ (see the Appendix); in the regions of interest to us we find $v_\tau \lesssim 5\,\mathrm{GeV}$ from

$$v_\tau = \frac{2\cos\theta_W}{g}\sqrt{m_\nu}\sqrt{|(M_Z^2/\mu)\,s_T - \beta M|} \qquad \text{(IV.B.2)}$$

where we define

$$\beta \equiv \frac{b}{1+(b-1)\cos^2\theta_W} = 0.81,$$
$$\tan\theta_V \equiv \frac{v_1}{v_2},\ c_V \equiv \cos\theta_V,\ s_V \equiv \sin\theta_V,\ c_T \equiv \cos(2\theta_V),\ s_T \equiv \sin(2\theta_V) \qquad \text{(IV.B.3)}$$

Let $\mathbf{A}$ be a diagonal matrix with entries $\frac{g}{\cos\theta_W}(T_{3L} - Q\sin^2\theta_W)$ for each of the gauge eigenstates,

$$\mathbf{A} = \frac{g}{\cos\theta_W}\,\mathrm{diag}(0,\ 0,\ \tfrac{1}{2},\ {}^{-}\tfrac{1}{2},\ \tfrac{1}{2}) \qquad \text{(IV.B.4)}$$

Then the effective coupling of Z^0 to $\bar{\nu}_\tau\,\chi_i^0$ is

$$A_i^{\mathrm{eff}} = \mathbf{q}_5^\dagger\,\mathbf{A}\,\mathbf{q}_i \qquad \text{(IV.B.5)}$$

and the branching ratio is

$$BR_i = 0.71\,(A_i^{\mathrm{eff}})^2\,\alpha_i^2\,(1-\frac{\alpha_i}{3})$$
$$\alpha_i \equiv 1-(m_i/M_Z)^2 \qquad \text{(IV.B.6)}$$

In terms of Feynman diagrams, $Z^0 \to \bar{\nu}_\tau \chi^0$ occurs through the diagrams of Fig. 23.

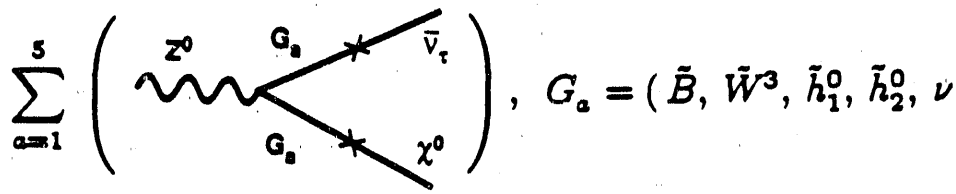

Figure 23: $Z^0 \to \bar{\nu}_\tau \chi^0$

The charged fermion mass matrix is:

$$(\omega^- \quad h_1^- \quad \tau^-) \begin{pmatrix} M & \sqrt{2}M_W c_V & 0 \\ \sqrt{2}M_W s_V & \mu & -m_\tau v_\tau / v_1 \\ g v_\tau / \sqrt{2} & 0 & m_\tau \end{pmatrix} \begin{pmatrix} \omega^+ \\ h_2^+ \\ \tau^c \end{pmatrix} \qquad \text{(IV.B.7)}$$

In addition to the usual mixing of winos and higgsinos, diagonalization of this matrix mixes τ^- with the negative charginos.* Regions of (μ, M) space are ruled out by requiring the charginos (except the τ) to be heavier than 40 GeV[43,44]; these masses are

$$m_i^2 = \tfrac{1}{2}(M^2 + \mu^2 + 2M_W^2) \pm \sqrt{\tfrac{1}{4}(M^2 + \mu^2 + 2M_W^2)^2 - (M_W^2 s_T - M\mu)^2} \qquad \text{(IV.B.8)}$$

with $m_1 > m_2$. A_i^{eff} for $Z^0 \to \tau^+ \chi^-$ is calculated as for the neutralinos, though now we can write it explicitly:

$$A_{1,2}^{\text{eff}} = \frac{g^2}{2\sqrt{2}\cos\theta_W} \frac{v_\tau \mu}{M_W^2 s_T - M\mu} \begin{pmatrix} -\cos\phi_- \\ \sin\phi_- \end{pmatrix} \qquad \text{(IV.B.9)}$$

where[45]

$$\tan(2\phi_-) = 2\sqrt{2}M_W(\mu c_V + M s_V)/(M^2 - \mu^2 + 2M_W^2 c_T) \qquad \text{(IV.B.10)}$$

The branching ratio is again given by eq. (IV.B.6).

---

* Rotation of τ^c is suppressed by m_τ/M, and the physical τ mass differs from m_τ by $\mathcal{O}(m_\tau v_\tau^2/M^2)$. The effect on tau physics is negligible.

C. BRANCHING RATIOS

We fix $\tan\theta_V = 1/4$, and plot branching ratio contours in the (μ, M) plane. The region ruled out by an excessively light chargino [see eq. (IV.B.8)] is shaded. The region allowing observable cascade decays not involving the neutrino, *e.g.*

$$\begin{aligned} Z^0 &\to \chi_4^0 \chi_3^0 \\ &\hookrightarrow \chi_4^0 f \bar{f} \end{aligned} \qquad \text{(IV.C.1)}$$

is not shown, but can be found in refs. [44,46]. Branching ratios for $Z^0 \to \bar{\nu}_\tau \chi^0$ are shown in Fig. 24, while those for $Z^0 \to \tau^+ \chi^-$ are shown in Fig. 25. Where several mass eigenstates are lighter than M_Z, their branching ratios have been added.

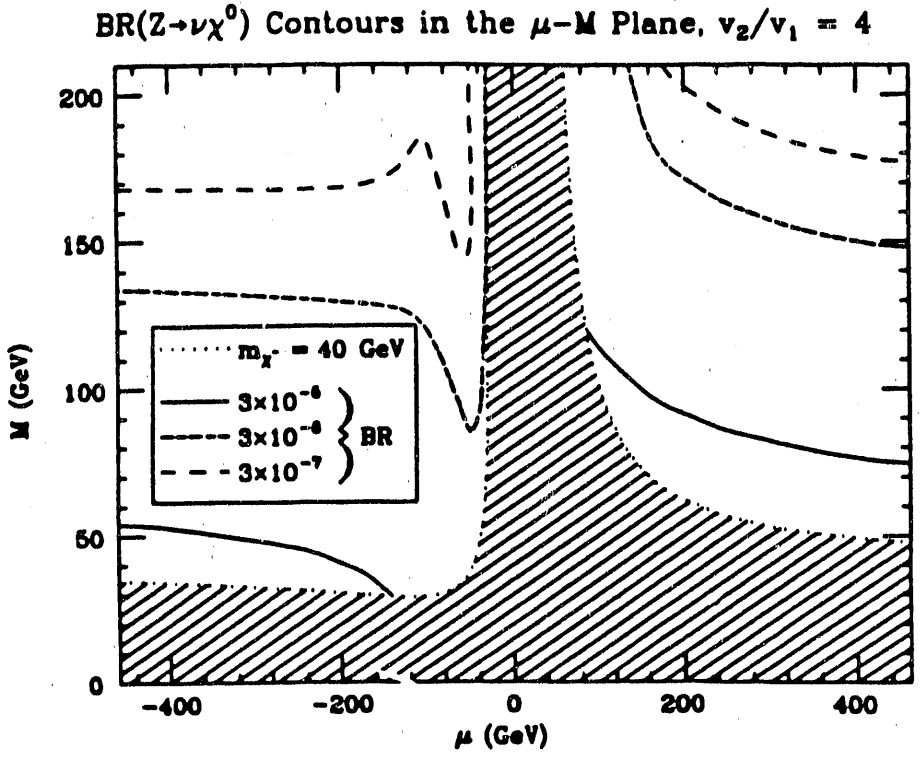

Figure 24: Branching Ratio $Z^0 \to \bar{\nu}_\tau \chi^0$

We note that models with additional particle content could increase the size of the mass matrix (IV.B.1), preserving the neutrino-neutralino mixing but leaving a

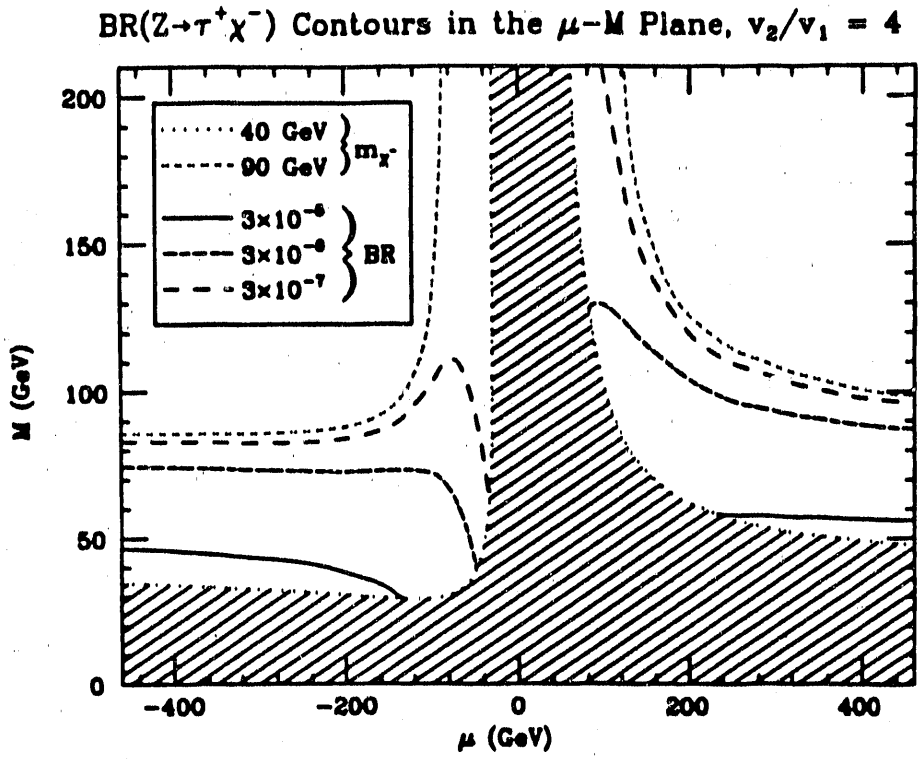

Figure 25: Branching Ratio $Z^0 \rightarrow \tau^+ \chi^-$

massless eigenstate. Then v_τ would not be so tightly restricted, and the branching ratios could be larger than we predict here.

D. SIGNATURES

Neutralinos and charginos may decay either through the QD^cL term or through their mixing with leptons. We consider these two cases separately.

1. 2 b-Jet Decays

Models with explicit R_P violation and a fairly light squark predict the χ^0 and χ^- will decay through the $Q_3 D_3^c L_3$ term, which arose from an $L \leftrightarrow h_1$ rotation on the b mass term. Assuming t's are not kinematically allowed in the final state, χ^0 and χ^- decay as in Fig. 26, $\chi^0 \rightarrow b\bar{b}\nu_\tau$ and $\chi^- \rightarrow b\bar{b}\tau^-$.

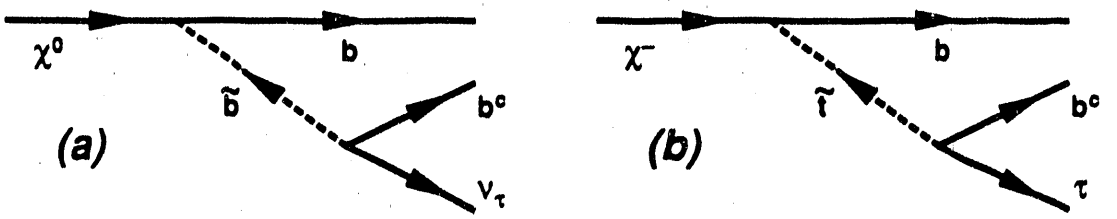

Figure 26: a) $\chi^0 \rightarrow b\bar{b}\nu_\tau$, b) $\chi^- \rightarrow b\bar{b}\tau^-$

Thus the primary signatures are:

$$\begin{array}{ll} Z^0 \rightarrow \bar{\nu}_\tau \chi^0 & Z^0 \rightarrow \tau^+ \chi^- \\ \quad \hookrightarrow b\bar{b}\nu_\tau & \quad \hookrightarrow b\bar{b}\tau^- \end{array} \qquad \text{(IV.D.1)}$$

The first is characterized by two b-jets with a large amount of missing mass. The average jet energy is larger than for the cascade decays of eq. (IV.C.1). Background for this signature comes from Fig. 27, but this Standard-Model diagram produces jets of other flavors equally often. Thus, a predominance of b-jets signals neutralino production.

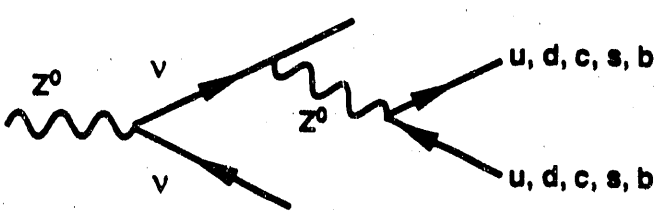

Figure 27: Background for 2-Jet Decays with Missing Mass

The second has two b-jets and two τ's. This signature is more challenging than the previous one, since it has little missing energy and momentum, and has four secondary vertices.

2. Decays From χ-L Mixing

In models without a QD^cL term, or in which squarks are very heavy, χ^0 and χ^- decay through their mixing with L, as in Fig. 28.

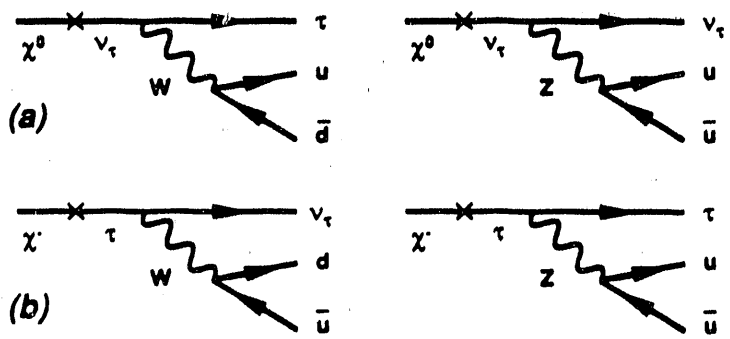

Figure 28: a) χ^0 Decays, b) χ^- Decays

Thus the primary signatures are:

$$\begin{array}{cccc} Z^0 \to \bar{\nu}_\tau \chi^0 & Z^0 \to \tau^+ \chi^- & Z^0 \to \bar{\nu}_\tau \chi^0 & Z^0 \to \tau^+ \chi^- \\ \hookrightarrow u\bar{d}\tau^- & \hookrightarrow d\bar{u}\nu_\tau & \hookrightarrow u\bar{u}\nu_\tau & \hookrightarrow u\bar{u}\tau^- \end{array} \qquad \text{(IV.D.2)}$$

where (u, d) can be replaced by other flavors or by leptons.

The first two are characterized by two jets and a τ, with a missing energy but low missing mass. The third and fourth are similar to the signatures of the previous subsection (and subject to the same background, Figure 27), but without the characteristic b-jet dominance.

E. CONCLUSIONS

If R-parity is violated and $\tilde{\nu}_\tau$ takes a vev, Z^0 decays involving a single neutralino or chargino can occur with branching ratios large enough to be seen at LEP I. χ^0 and χ^- subsequently decay to either b-jets and leptons, or jets and leptons, depending

on the model. The decay $Z^0 \to 2$ b-jets + missing mass, is particularly distinctive. If $\frac{1}{2}M_Z < m_\chi < M_Z$, these rare Z^0 decays may be the best way to observe neutralinos and charginos.

F. APPENDIX: ν MASS LIMITS

Standard cosmology rules out a stable 35 MeV ν_τ which annihilates predominantly through the Z^0. However, unstable 35 MeV ν_τ's produced in supernovas would decay and flood the galaxy with characteristic photons (511 keV from $\nu_\tau \to e^+e^-\nu_\mu$, or 17.5 MeV from $\nu_\tau \to \nu_e\gamma$). Below we give a few ways to circumvent these arguments and allow a 35 MeV neutrino:

1. Make the decay $\nu_\tau \to e^+e^-\nu_\mu$ occur very rapidly, with lifetime less than 1000 s. Then the decays occur within the supernova, and the photons are not detected from Earth. This increases the predicted supernova luminosity; however, since few 35 MeV ν_τ's are produced in the 3.5 MeV neutrinosphere, a small window may exist here. This idea also requires large violation of both τ- and μ-number: the coefficients of $C^{ijk}L_iL_jE^c_k$ would need to satisfy $C^{131} \times C^{121} \geq 4 \times 10^{-5}$.

2. Make ν_τ stable, and alter the standard cosmological picture. For example, let the universe reheat after inflation to only a few MeV. Then ν_τ's do not overclose the universe; they could even be the cold dark matter. This idea requires low-temperature baryogenesis[47].

3. Make ν_τ stable, and enhance the $\nu_\tau - \bar{\nu}_\tau$ annihilation rate by introducing a singlet Majoron M, the Goldstone bosons of broken lepton number.[48] Then $\nu_\tau\bar{\nu}_\tau \to MM$ prevents overclosure, as noticed by Carlson and Hall[49], and makes ν_τ a dark matter candidate. We will present a supersymmetric singlet Majoron model which links R_P and L-breaking in a future paper.[34]

V. RULING OUT LARGE SNEUTRINO VEVS

Suddenly, as rare things will, it vanished.
– "One Word More" (Robert Browning)

A. INTRODUCTION

In supersymmetric models with minimal field content, it is quite likely that the tau sneutrino acquire a large vacuum expectation value.[30,31] This occurs because the radiative mechanism which gives vevs to the Higgs doublets* causes $v_2 > v_1$. This triggers a negative mass-squared for the sneutrinos via the D^2 term in the potential $\propto (v_2^* v_2 - v_1^* v_1 - \tilde{\nu}^* \tilde{\nu})^2$. Smaller radiative corrections further depress the mass-squared of the tau sneutrino, ensuring that it is the only sneutrino with a vev. This is fortunate, since tau sneutrino vevs are the least constrained.

We showed in eq. (IV.B.2) that for most values of M (the supersymmetry-breaking wino mass) and μ (the supersymmetric $h_1 h_2$ coupling), $\langle \tilde{\nu}_\tau \rangle$ is constrained to be small because it mixes the tau neutrino with the zino, giving the tau neutrino a mass. For small $\langle \tilde{\nu}_\tau \rangle$ this mass is

$$m_\nu \approx \left(\frac{g \langle \tilde{\nu}_\tau \rangle}{\sqrt{2} \cos \theta_W} \right)^2 \frac{\mu}{M_Z^2 s_{2\beta} - .81 M \mu} \qquad \text{(V.A.1)}$$

where

$$s_{2\beta} \equiv \sin(2\beta), \quad \tan\beta \equiv v_2/v_1', \quad v_1' \equiv \sqrt{v_1^2 + \langle \tilde{\nu}_\tau \rangle^2} \qquad \text{(V.A.2)}$$

Limits on the tau neutrino mass ($m_\nu < 35\,\text{MeV}$) constrain $\langle \tilde{\nu}_\tau \rangle \lesssim 10\,\text{GeV}$ unless $M \gtrsim 1\,\text{TeV}$ or $|\mu| \lesssim 10\,\text{GeV}$.**

The above mechanism for the generation of a tau sneutrino vev suggests either $\langle \tilde{\nu}_\tau \rangle = 0$ or $\langle \tilde{\nu}_\tau \rangle \sim v_1, v_2$; there is no reason for it to be small. Furthermore, making

*h_1 couples to down quarks, and h_2 to up quarks. In this chapter, $v_1 \equiv \langle h_1^0 \rangle$ and $v_2 \equiv \langle h_2^0 \rangle$.

**Regions of small μ and large M are disallowed, since they have a light chargino.

$M > 1$ TeV also requires a fine tuning. The last possibility is that μ is much less than the other mass parameters in the low-energy theory. This is an attractive possibility: μ is the only supersymmetric mass term in the model, and has no fundamental reason to be linked to the scale of supersymmetry breaking. Models with small μ and large $\langle\tilde{\nu}_\tau\rangle$ have been constructed[28]. It is quite remarkable that they can be made realistic: in the limit $\mu \to 0$ not only is there a light state to be identified as the tau neutrino $\nu_\tau^{\rm phys} = c\nu + s\tilde{h}_1^0$, but its SU(2) partner $\tau^{\rm phys} = c\tau + s\tilde{h}_1^-$ is also light. These models are of considerable interest as an example of how the minimal low-energy supersymmetric model can lead to the unusual phenomenology of broken R-parity[27-34].

There are many variant models with small μ and large $\langle\tilde{\nu}_\tau\rangle$, dealing in various ways with such questions as axions, Majorons, and cosmological domain walls. As we saw in Chapter III, models with explicit R_P violation can also generate a large sneutrino vev, from the rotation $L \leftrightarrow h_1$ needed to eliminate Lh_2 from the superpotential.[33] Since we consider only the higgsino/gaugino sector, we will show that all such models with the usual neutralino and chargino mass matrices (in the small μ limit) are excluded by LEP data and gluino searches.

B. THE $\mu = 0$ MODEL

When $\mu = 0$, we can rotate the lepton and Higgs superfields so that in the rotated basis $\langle\tilde{\nu}_\tau\rangle = 0$; the R_P violation then shows up in terms like QD^cL and LLE^c. The chargino and neutralino mass matrices are the usual ones with $\mu = 0$ (and $v_1 \to v_1'$). One massless neutralino ($\nu_\perp \equiv s_\beta\tilde{h}_1^0 + c_\beta\tilde{h}_2^0$) occurs, while the remaining neutralino mass matrix is:

$$(\tilde{\gamma}\ \ \tilde{z}\ \ \eta)\begin{pmatrix}(bc_W^2+s_W^2)M & (1-b)s_Wc_WM & 0\\ (1-b)s_Wc_WM & (bs_W^2+c_W^2)M & M_Z\\ 0 & M_Z & 0\end{pmatrix}\begin{pmatrix}\tilde{\gamma}\\ \tilde{z}\\ \eta\end{pmatrix} \qquad \text{(V.B.1)}$$

where $\eta \equiv c_\beta \tilde{h}_1^0 - s_\beta \tilde{h}_2^0$. We will assume gaugino masses scale roughly as couplings, so the gluino mass $M_{\tilde{g}} = 3.65M$, and the bino mass $M_{\tilde{B}} = bM$ where $b = 0.49$. For $M \lesssim M_Z$ the lightest eigenstate χ^0 is mostly photino, and has mass $m_\chi \approx (s_W^2 + bc_W^2)M = 0.61M$.

We use the following constraints, shown in Fig. 29:

- Z^0 width. $\nu_\perp$'s contribution to the Z^0 width depends on $\tan\beta$. LEP data giving $N_\nu \leq 3.25$ at the 95% confidence limit[1] restricts $s_{2\beta} \geq 0.87$, or $0.58 \leq \tan\beta \leq 1.73$, as shown.

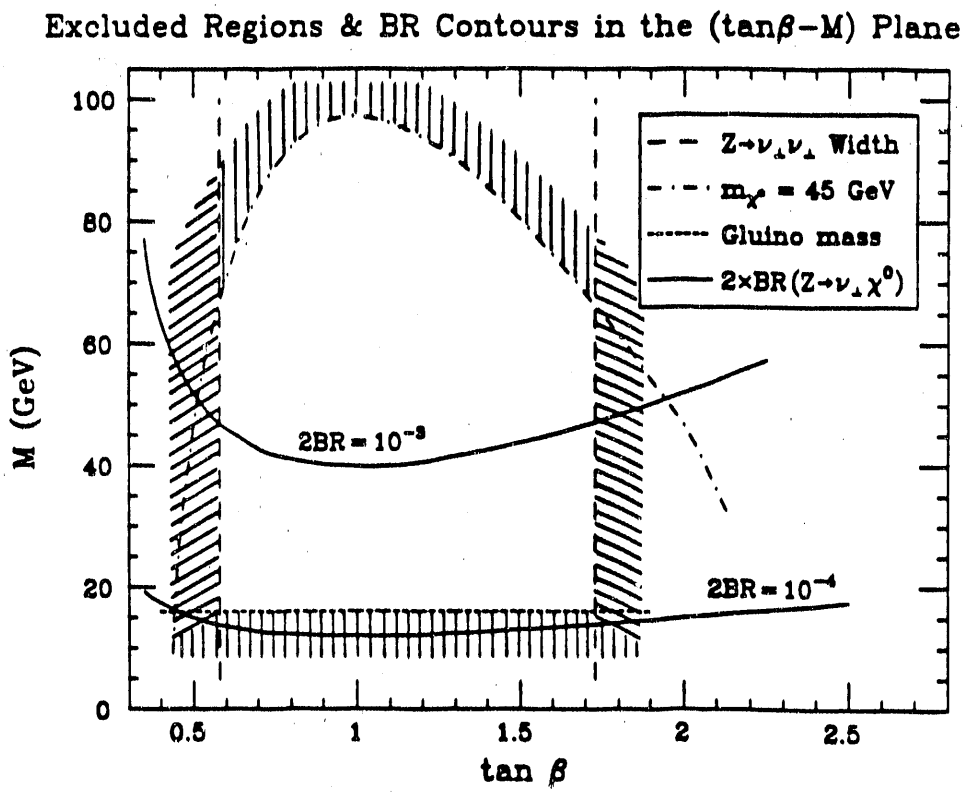

Figure 29: Excluded Regions & BR Contours in the $(\tan\beta - M)$ Plane

- Chargino mass limits. LEP data[50] shows the lightest chargino must be heavier than $M_Z/2$, giving

$$\tfrac{1}{2}M^2 + M_W^2 - \sqrt{(\tfrac{1}{2}M^2 + M_W^2)^2 - (s_{2\beta}M_W^2)^2} > (\tfrac{1}{2}M_Z)^2 \qquad \text{(V.B.2)}$$

This eliminates large M.

- Gluino mass limits. Gluinos produced in hadron colliders can decay via the diagrams of Fig. 30; the radiative diagram (b) has a significant branching ratio[51,52] for $\mu \approx 0$ and $M \lesssim 15\,\text{GeV}$. While Tevatron's published limit[5] $M_{\tilde{g}} > 73\,\text{GeV}$ ($M > 20\,\text{GeV}$) assumes only decay (a) with a stable χ^0 (photino), we must account both for the subsequent decay[53] of the χ^0 (Fig. 31), and for the radiative decay of Fig. 30(b). To calculate the relative rates of decays (a) and (b), we used the formulas of ref. [51], with conservative values $m_t = 89\,\text{GeV}$[4] and $\ln(m_t/m_{\tilde{q}}) = 0$. A Monte Carlo simulation[54] gave $M \geq 16\,\text{GeV}$ at the 90% confidence level, assuming $M_{\tilde{g}} = 3.65M$.

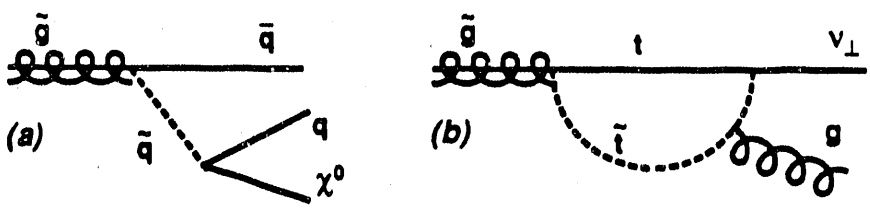

Figure 30: Gluino Decay

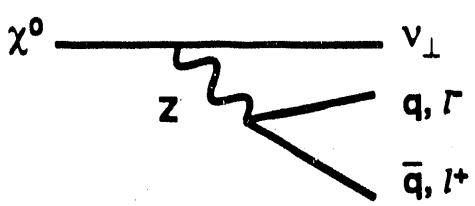

Figure 31: χ^0 Decay

- Rare Z^0 decays:

$$\begin{array}{l} Z^0 \to \bar{\nu}_\perp \chi^0 \\ \qquad\quad \hookrightarrow \nu_\perp q\bar{q} \end{array} \tag{V.B.3}$$

and its CP conjugate. The branching ratio can be calculated from eq. (IV.B.6), giving roughly

$$2 \times \mathrm{BR} \approx 1.4 \times 10^{-4} \left(\frac{M}{16\,\mathrm{GeV}}\right)^2 \left(\frac{s_{2\beta}}{.87}\right)^2 \tag{V.B.4}$$

This decay is distinguished by two jets (or sometimes l^+l^-) with missing energy and missing mass. Higgs searches at LEP[2] have looked for a similar signal from $Z^0 \to h^0\nu\bar{\nu}$. Applying their cuts to our process, we find the remaining region of Fig. 29 ruled out at the 90% confidence level.

C. MODELS WITH $\mu \approx 0$

When $\mu \neq 0$ the analysis is qualitatively similar, but more complicated in detail. Rotating away the sneutrino vev now introduces an Lh_2 coupling, with coefficient $\mu\langle\tilde{\nu}_\tau\rangle/v_1'$. The neutralino/neutrino and chargino/tau mass matrices are 5×5 and 3×3, respectively, with the additional parameters μ and $\langle\tilde{\nu}_\tau\rangle$. The physical tau and tau neutrino contain small admixtures of SU(2) triplets and singlets. The $\nu_\perp$ is no longer massless, and will decay through the QD^cL or LLE^c operators. These additional considerations made a numerical analysis necessary.

We performed a computer scan of $(\tan\beta, M, \mu, \langle\tilde{\nu}_\tau\rangle)$ space near $\mu = 0$, requiring a tau neutrino mass under 35 MeV [eq. (V.A.1)], and applying the same constraints as in the previous section. We found that all points with $\langle\tilde{\nu}_\tau\rangle \geq 10\,\mathrm{GeV}$ could be eliminated, again at the 90% confidence level.

D. CONCLUSIONS

We have considered models with the minimal higgsino/gaugino sector, and the usual gaugino mass ratios. Current LEP data, combined with gluino mass limits, rules out any such model with $\mu \approx 0$ and a large sneutrino vev ($\langle \tilde{\nu}_\tau \rangle \geq 10\,\mathrm{GeV}$), at the 90% confidence level. Neutrino mass limits disallow large sneutrino vevs everywhere else except for unnaturally large M, for which

$$\langle \tilde{\nu}_\tau \rangle \lesssim (10\,\mathrm{GeV})\sqrt{\frac{M}{1\,\mathrm{TeV}}} \qquad \text{(V.D.1)}$$

Therefore, unless the supersymmetry scale is unnaturally high, large sneutrino vevs are experimentally ruled out for these models.

VI. SUMMARY: TODAY'S CHALLENGE

These are the days of miracle and wonder.

– Paul Simon, "The Boy in the Bubble"

In this dissertation we have explored several models of new physics, involving a new $U(1)'$ gauge group, and supersymmetry without R-parity (R_P).

All models with an extra $U(1)'$ gauge group, including most Grand Unified Theories, present an appealing dark matter candidate, a fermion which couples to matter only through the exchange of a heavy Z'. Here cosmology allows us to compute a relation between the particle's mass and its cross-section with a germanium detector. If a dark matter candidate is detected, and it satisfies that relation, we will have learned a great deal about the $U(1)'$ sector.

Supersymmetric models usually impose a discrete symmetry, R_P, to conserve lepton- and baryon-number. The phenomenology of such models has been well studied, largely making use of a stable lightest superpartner (LSP). Viable models without R_P can be built, and it is worthwhile understanding their signatures, notably rare Z^0 decays. On the other hand, many constraints exist on these models; we have shown how one class of models with a large sneutrino vev is already ruled out.

There are many theoretical reasons to believe in physics beyond the Standard Model, and a wealth of data discouraging that belief. While we can almost certainly expect to find interesting new physics at the SSC, our present challenge is to understand what models are allowed by the available data, and to be prepared to recognize the signatures of those models.

REFERENCES:

There is nothing so absurd but some philosopher has said it.

– "De Divinatione" (Cicero)

[1] 1990 Particle Data Book, to be published in *Phys. Lett.* **B**;
The previous volume is in *Phys. Lett.* **204B**:1 (1988).

[2] Aleph Collab., preprint CERN-EP/90-16 (1990).

[3] G. Costa, J. Ellis, G.L. Fogli, D.V. Nanopoulos & F. Zwirner, *Nucl. Phys.* **B297**:244 (1988).

[4] CDF Collab., *Phys. Rev. Lett.* **64**:142 (1990) gives $m_t > 77\,\mathrm{GeV}$, and preliminary analysis (P. Tipton, LBL talk 3/22/90) gives $m_t > 89\,\mathrm{GeV}$.

[5] CDF Collab., *Phys. Rev. Lett.* **62**:1825 (1989);
J. Freeman, preprint FERMILAB-Conf-89/148-E (1989);
see also UA2 Collab., *Phys. Lett.* **235B**:363 (1990).

[6] D.O. Caldwell, R.M. Eisberg, D.M. Grumm, M.S. Witherell, B. Sadoulet, F.S. Goulding & A.R. Smith, "Laboratory Limits on Galactic Cold Dark Matter" (unpublished);
D.O. Caldwell, R.M. Eisberg, F.S. Goulding, D.M. Grumm, B. Sadoulet, A.R. Smith & M.S. Witherell, in *Dark Matter: Proc. of the XXIIIrd Rencontre de Moriond*, Les Arcs, Savoie, France, March 8–15, 1988, edited by J. Audouze & J. Tran Thanh Van;
B. Sadoulet, private communication.

[7] S.P. Ahlen, F.T. Avignone III, R.L. Brodzinski, A.K. Drukier, G. Gelmini & D.N. Spergel, *Phys. Lett.* **195B**:603 (1987).

[8] A. Drukier & L. Stodolsky, *Phys. Rev.* **D30**:2295 (1984).

[9] M.B. Green, J.H. Schwarz & E. Witten, *Superstring Theory* (Cambridge University Press, 1987);
J.P. Derendinger, L.E. Ibáñez & H.P. Nilles, *Nucl. Phys.* **B267**:365 (1986);
E. Witten, *Nucl. Phys.* **B258**:75 (1985);
S. Hsu, private communication.

[10] H. Georgi & S.L. Glashow, *Phys. Rev. Lett.* **32**:438 (1974).

[11] A. De Rújula, H. Georgi & S.L. Glashow, *Phys. Rev. Lett.* **45**:413 (1980);
S.M. Barr, *Phys. Lett.* **112B**:219 (1982).

[12] I. Antoniadis, J. Ellis, J.S. Hagelin & D.V. Nanopoulos, *Phys. Lett.* **194B**:231 (1987), discuss a $\overline{\mathrm{SU}(5)}$ model with only dimension four (trilinear) terms in the superpotential, and imposes a discrete symmetry ($H \rightarrow -H$) to eliminate $\mathrm{R_P}$-violating terms at this level. However, non- (and super-) renormalizable terms obeying this symmetry would violate B and L badly (e.g. $M_P^{-3}(H\bar{H})HFF\bar{f}$) as well as destroying the flat directions of the theory (e.g. $M_P F\bar{H}$ or $M_P^{-1}(H\bar{H})^2$). Their model also requires four singlet fields ϕ_m, three driving the neutrino seesaw mechanism by marrying the ν_i^c, and one taking a weak-scale vev to mix h and $\bar{h}$. We achieve these goals through the additional non-renormalizable terms in our superpotential.

[13] J. Rizos & K. Tamvakis, *Phys. Lett.* **212B**:176 (1988).

[14] T.G. Rizzo, NASA-Ames preprint IS-J-3091 (June 1988).

[15] L.E. Ibáñez & J. Mas, *Nucl. Phys.* **B286**:107 (1987).

[16] J. Ellis, K. Enqvist, D.V. Nanopoulos & F. Zwirner, *Nucl. Phys.* **B276**:14 (1986);
E. Cohen, J. Ellis, K. Enqvist & D.V. Nanopoulos, *Phys. Lett.* **165B**:76 (1985).

[17] J.C. Pati & A. Salam, *Phys. Rev.* **D8**:1240 (1973).

[18] K. Griest & B. Sadoulet, in *Proc. of the Second Particle Astrophysics School on Dark Matter*, Erice, Italy, 1988 (FERMILAB-Conf-89/57-A).

[19] B.W. Lee & S. Weinberg, *Phys. Rev. Lett.* **39**:165 (1977);
P. Hut, *Phys. Lett.* **69B**:85 (1977);
K. Sato & M. Kobayashi, *Prog. Theor. Phys.* **58**:1775 (1977);
M.I. Vysotskii, A.D. Dolgov & Ya.B. Zel'dovich, *Pis'ma Zh. Eksp. Teor. Fiz.* **26**:200 (1977) [*JETP Lett.***26**:188 (1977)];
D.A. Dicus, E.W. Kolb & V.L. Teplitz, *Phys. Rev. Lett.* **39**:168 (1977);
G.L. Kane & I. Kani, *Nucl. Phys.* **B277**:525 (1986);
E.W. Kolb & K.A. Olive, *Phys. Rev.* **D33**:1202 (1986) & **D34**:2531 (1986).

[20] An interesting U(1)′ cosmion model is developed by G.G. Ross & G.C. Segrè, *Phys. Lett.* **B197**:45 (1987), by allowing a particle-antiparticle asymmetry. Their U(1)′, with $(\beta, \lambda, \kappa) = (2, -2, 1)$, allows for a very light Z′ (65 GeV) and a large G'. A large scattering cross-section for ψ off of helium provides for capture by the sun, and solves the solar neutrino problem. Under our assumption of symmetry, the annihilation cross-section would also be large, and these ψ's could not close the universe. However, asymmetry alters the Lee-Weinberg result, so an asymmetric ψ could cool the sun and close the universe.

[21] K. Olive, D. Schramm & G. Steigman, *Nucl. Phys.* **B180[FS2]**:497 (1981).

[22] M.W. Goodman & E. Witten, *Phys. Rev.* **D31**:3059 (1985).

[23] The annihilation cross-section for $\psi\bar{\psi} \rightarrow Z'Z'$ in eqs. (II.C.17) & (II.C.30) agrees with a more general calculation done by K. Griest & M. Kamionkowski (unpublished).

[24] K. Griest, *Phys. Rev.* **D38**:2357 (1988);
K. Freese, J. Frieman & A. Gould, *Phys. Rev.* **D37**:3388 (1988);

Kim Griest, private communication.

Since the momentum transfer becomes independent of m_ψ for large m_ψ, the coherence factor $\eta_C \to 0.3$ in this limit.

[25] E. Jenkins, *Phys. Lett.* **192B**:219 (1987);
F. Del Aguila, M. Quirós & F. Zwirner, *Nucl. Phys.* **B284**:530 (1987);
F. Del Aguila, M. Quirós & F. Zwirner, *Nucl. Phys.* **B287**:419 (1987).

[26] K. Enqvist, K. Kainulainen & J. Maalampi, *Nucl. Phys.* **B316**:456 (1989).
Enqvist *et al.* independently derive m_ψ limits from $M_{Z'}$ limits [our eq. (II.E.1)]. For symmetry $S^{(3)}$, using $M_{Z'} \geq 156\,\mathrm{GeV}$, $\Omega h_0^2 \leq \frac{1}{2}$, and fixed $g_1' = g_1$, they find $m_\psi \geq 17\,\mathrm{GeV}$, which is consistent with our result. They do not consider the cross-section in a germanium detector; however, they do examine more carefully the effects of $Z^0 - Z'$ mixing, and they have a good discussion of solar capture. We thank K. Griest for pointing this work out to us.

[27] S. Dimopoulos & L.J. Hall, *Phys. Lett.* **207B**:210 (1987).

[28] J. Ellis, G. Gelmini, C. Jarlskog, G.G. Ross & J.W.F. Valle, *Phys. Lett.* **150B**: 142 (1985).

[29] H. König, *Z. Phys.* **C44**:401 (1989).

[30] G. Ross & J. Valle, *Phys. Lett.* **151B**:375 (1985).

[31] C.S. Aulakh & R.N. Mohapatra, *Phys. Lett.* **119B**:136 (1982).

[32] F. Zwirner, *Phys. Lett.* **132B**:103 (1983);
I.H. Lee, *Nucl. Phys.* **B246**:120 (1984);
S. Dawson, *Nucl. Phys.* **B261**:297 (1985);
R. Barbieri & A. Masiero, *Nucl. Phys.* **B267**:679 (1986);
S. Dimopoulos, R. Esmailzadeh, L.J. Hall & G.D. Starkman, SLAC-PUB-4797 (Sep. 1988), submitted to *Phys. Rev. D*;

D. Brahm & L.J. Hall, *Phys. Rev.* **D40**:2449 (1989);

L. Hall, Preprint LBL-28347 (1990), to be published in Brief Reports of *J. Mod. Phys.*

[33] L.J. Hall & M. Suzuki, *Nucl. Phys.* **B231**:419 (1984).

[34] D. Brahm, L.J. Hall & S. Hsu, "A Supersymmetric Singlet Majoron Model", LBL-28208 (Dec. 1989), work in progress.

[35] M.C. Bento, L.J. Hall & G.G. Ross, *Nucl. Phys.* **B292**:400 (1987).

[36] H. Georgi, H. Quinn & S. Weinberg, *Phys. Rev. Lett.* **33**:451 (1974).

[37] A.J. Buras, J. Ellis, M.K. Gaillard & D.V. Nanopoulos, *Nucl. Phys.* **B135**:66 (1978).

[38] S. Dimopoulos & F. Wilczek, *Erice 81 Proceedings* (ed. A. Zichichi) 237.

[39] M. Claudson, L.J. Hall & I. Hinchliffe, *Nucl. Phys.* **B228**:501 (1983), Fig. 5.

[40] M. Drees, *Phys. Lett.* **206B**:265 (1988).

[41] M.B. Wise, *The Santa Fe TASI-87* (ed. R. Slansky & G. West) 787;

A. Chamseddine, R. Arnowitt & P. Nath, *Phys. Rev. Lett.* **49**:970 (1982);

R. Barbieri, S. Ferrara & C. Savoy, *Phys. Lett.* **119B**:343 (1982);

L. Ibanez, *Phys. Lett.* **118B**:73 (1982);

H.P. Nilles, *Phys. Lett.* **115B**:1973 (1982);

L.J. Hall, J. Lykken & S. Weinberg, *Phys. Rev.* **D27**:2359 (1983).

[42] J. Ellis, J.S. Hagelin, S. Kelley & D.V. Nanopoulos, *Nucl. Phys.* **B311**:1 (1988).

[43] H. Baer, K. Hagiwara & X. Tata, *Phys. Rev.* **D38**:1485 (1988).

[44] G.F. Giudice & G. Ridolfi, *Z. Phys.* **C41**:447 (1988);

R. Barbieri, M. Frigeni & G.F. Giudice, *Nucl. Phys.* **B313**:725 (1989).

[45] H.E. Haber & G.L. Kane, *Physics Reports* **117**:75 (1985).

[46] J. Ellis, J.S. Hagelin, D.V. Nanopoulos & M. Srednicki, *Phys. Lett.* **127B**:233 (1983);

R. Barbieri, G. Gamberini, G.F. Giudice & G. Ridolfi, *Phys. Lett.* **195B**:500 (1987);

R. Barbieri, G. Gamberini, G.F. Giudice & G. Ridolfi, *Nucl. Phys.* **B296**:75 (1988) and references therein.

[47] S. Dimopoulos & L.J. Hall, *Phys. Lett.* **196B**:135 (1987).

[48] Y. Chikashige, R. Mohapatra & R. Peccei, *Phys. Lett.* **98B**:265 (1981).

[49] E.D. Carlson & L.J. Hall, *Phys. Rev.* **D40**:3187 (1989).

[50] L3 Collab., *Phys. Lett.* **233B**:530 (1989);

Aleph Collab., *Phys. Lett.* **236B**:86 (1990).

[51] R. Barbieri, G. Gamberini, G. Giudice, & G. Ridolfi, *Nucl. Phys.* **B301**:15 (1988), esp. Fig. 6.

[52] E. Ma and G. Wong, *Mod. Phys. Lett.* **A3**:1561 (1988).

[53] H. Baer, X. Tata, and J. Woodside, *Phys. Rev.* **D41**:906 (1990).

[54] We ran a modified version of a Monte Carlo routine by R.M. Barnett.

END

DATE FILMED

11 / 21 / 90